

Breaking Eight-fold Degeneracies in Neutrino *CP* Violation, Mixing, and Mass Hierarchy

V. Barger¹, D. Marfatia² and K. Whisnant³

¹*Department of Physics, University of Wisconsin, Madison, WI 53706, USA*

²*Department of Physics, Boston University, Boston, MA 02215, USA*

³*Department of Physics and Astronomy, Iowa State University, Ames, IA 50011, USA*

Abstract

We identify three independent two-fold parameter degeneracies (δ, θ_{13}) , $\text{sgn}(\delta m_{31}^2)$ and $(\theta_{23}, \pi/2 - \theta_{23})$ inherent in the usual three-neutrino analysis of long-baseline neutrino experiments, which can lead to as much as an eight-fold degeneracy in the determination of the oscillation parameters. We discuss the implications these degeneracies have for detecting *CP* violation and present criteria for breaking them. A superbeam facility with a baseline at least as long as the distance between Fermilab and Homestake (1290 km) and a narrow band beam with energy tuned so that the measurements are performed at the first oscillation peak can resolve all the ambiguities other than the $(\theta_{23}, \pi/2 - \theta_{23})$ ambiguity (which can be resolved at a neutrino factory) and a residual $(\delta, \pi - \delta)$ ambiguity. However, whether or not *CP* violation occurs in the neutrino sector can be ascertained independently of the latter two ambiguities. The $(\delta, \pi - \delta)$ ambiguity can be eliminated by performing a second measurement to which only the $\cos\delta$ terms contribute. The hierarchy of mass eigenstates can be determined at other oscillation peaks only in the most optimistic conditions, making it necessary to use the first oscillation maximum. We show that the degeneracies may severely compromise the ability of the proposed SuperJHF-HyperKamiokande experiment to establish *CP* violation. In our calculations we use approximate analytic expressions for oscillation probabilities that agree with numerical solutions with a realistic Earth density profile.

I. INTRODUCTION

The up/down asymmetry of the neutrino flux (originating from cosmic ray interactions with the atmosphere) at SuperKamiokande is now a 10σ effect. A compelling interpretation of this result is that neutrinos have mass and oscillate from one flavor to another. The atmospheric neutrino deficit is explained as a consequence of $\nu_\mu \rightarrow \nu_\tau$ oscillations with almost maximal amplitude and mass-squared difference, $\delta m_{31}^2 \sim 3 \times 10^{-3} \text{ eV}^2$ [1]. The K2K experiment [2] with a baseline of 250 km has preliminary results that are in agreement with this interpretation. Oscillations of ν_μ to ν_e as an explanation of the atmospheric anomaly are ruled out by the CHOOZ [3] and Palo Verde [4] reactor experiments, which place a bound on the amplitude smaller than 0.1 at the 95% C.L. in the δm_{31}^2 region of interest. The MINOS [5], ICARUS [6] and OPERA [7] experiments are expected to come online in 2005 and study aspects of the oscillations at the atmospheric scale [8]. The low energy beam at MINOS will allow a very accurate determination of the leading oscillation parameters. ICARUS and OPERA should provide concrete evidence that $\nu_\mu \rightarrow \nu_\tau$ oscillations are responsible for the atmospheric neutrino deficit by identifying tau neutrino events.

Measurements of electron neutrinos from the Sun also provide strong evidence for neutrino oscillations. The flux of electron neutrinos from the Sun observed in several different experiments is smaller than the Standard Solar Model [9] (SSM) prediction by a factor of $1/3$ – $1/2$. The recent SNO charged-current measurements show that $\nu_e \rightarrow \nu_{\mu,\tau}$ oscillations explain the ν_e flux suppression relative to the SSM [10]. The solution with a large mixing angle (LMA) and small matter effects ($\delta m_{21}^2 \sim 5 \times 10^{-5} \text{ eV}^2$ and amplitude close to 0.8) has emerged as the most likely solution to the solar neutrino problem [11]. This solution will be tested decisively by the KamLAND reactor neutrino experiment [12].

There are several parameter degeneracies that enter the determination of the neutrino mixing matrix which can be removed only with future oscillation studies with superbeams or neutrino factories. See Table I for a sample of proposed baselines. A notable example is the U_{e3} ($=\sin\theta_{13} e^{-i\delta}$) element. Only an upper bound exists on θ_{13} , nothing is presently known about the CP phase δ , and the two always appear in combination in the mixing matrix. It is the breaking of such degeneracies that will be of concern to us in this work.

In Section II we identify all the potential parameter degeneracies in the mixing matrix. We restrict our attention to the 3×3 matrix that describes the mixing of active neutrinos, setting aside the possibility that the atmospheric, solar and LSND [13] data may require the existence of a fourth neutrino that is sterile. The parameter ambiguities are connected with

TABLE I. Baseline distances in km for some detector sites (shown in parentheses) for neutrino beams from Fermilab, Brookhaven, JHF, and CERN.

Fermilab	Beam source		
	Brookhaven	JHF	CERN
	350 (Cornell)	295 (Super-K)	150 (Frejus)
730 (Soudan)			730 (Gran Sasso)
1290 (Homestake)		1200 (Seoul)	
1770 (Carlsbad)	1720 (Soudan)		
		2100 (Beijing)	
2640 (San Jacinto)	2540 (Homestake)		
2900 (SLAC)	2920 (Carlsbad)		

not only neutrino mixing but also the neutrino mass pattern; we pay particular attention to the implication of these ambiguities for the detection of CP violation. In Section III, within the context of a superbeam experiment [14], we present methods by which all but one of these degeneracies can be resolved, and argue that the remaining ambiguity can be settled at a neutrino factory [15]. We also discuss the implications of the degeneracies on the proposed SuperJHF–HyperKamiokande experiment [16], which would have a 4 MW proton driver and a 1 Mt water cerenkov detector (40 times larger than SuperKamiokande). We summarize our results in Section IV. In an appendix we provide a complete set of approximate analytic expressions for the oscillation probabilities that are useful for superbeams and neutrino factories, and define their domain of validity by making comparisons with numerical solutions of the evolution equations.

II. PARAMETER DEGENERACIES

In this section we identify the three types of parameter degeneracies that can occur in the three–neutrino framework when $\nu_\mu \rightarrow \nu_e$ and $\bar{\nu}_\mu \rightarrow \bar{\nu}_e$ oscillation probabilities are used to extract the neutrino parameters. We use approximate formulas [17,18] for neutrino propagation in matter of constant density to illustrate the degeneracies. In each case we discuss the implications for detecting CP violation.

A. Oscillation probabilities in matter

The neutrino flavor eigenstates ν_α ($\alpha = e, \mu, \tau$) are related to the mass eigenstates ν_j ($j = 1, 2, 3$) in vacuum by

$$\nu_\alpha = \sum_j U_{\alpha j}^* \nu_j , \quad (1)$$

where U is a unitary 3×3 mixing matrix. The propagation of neutrinos through matter is described by the evolution equation [19,20]

$$i \frac{d\nu_\alpha}{dx} = \sum_\beta \left(\sum_j U_{\alpha j} U_{\beta j}^* \frac{m_j^2}{2E_\nu} + \frac{A}{2E_\nu} \delta_{\alpha e} \delta_{\beta e} \right) \nu_\beta , \quad (2)$$

where $x = ct$ and $A/2E_\nu$ is the amplitude for coherent forward charged-current ν_e scattering on electrons,

$$A = 2\sqrt{2} G_F N_e E_\nu = 1.52 \times 10^{-4} \text{ eV}^2 Y_e \rho (\text{g/cm}^3) E_\nu (\text{GeV}) , \quad (3)$$

Here N_e is the electron number density, which is the product of the electron fraction $Y_e(x)$ and matter density $\rho(x)$. In the Earth’s crust and mantle the average matter density is typically 3–5 g/cm³ and $Y_e \simeq 0.5$. The propagation equations can be re-expressed in terms of mass-squared differences

$$i \frac{d\nu_\alpha}{dx} = \sum_\beta \frac{1}{2E_\nu} \left(\delta m_{31}^2 U_{\alpha 3} U_{\beta 3}^* + \delta m_{21}^2 U_{\alpha 2} U_{\beta 2}^* + A \delta_{\alpha e} \delta_{\beta e} \right) , \quad (4)$$

where $\delta m_{jk}^2 \equiv m_j^2 - m_k^2$. The neutrino mixing matrix U can be specified by 3 mixing angles $(\theta_{23}, \theta_{12}, \theta_{13})$ and a CP -violating phase δ . We adopt the parameterization

$$U = \begin{pmatrix} c_{13}c_{12} & c_{13}s_{12} & s_{13}e^{-i\delta} \\ -c_{23}s_{12} - s_{13}s_{23}c_{12}e^{i\delta} & c_{23}c_{12} - s_{13}s_{23}s_{12}e^{i\delta} & c_{13}s_{23} \\ s_{23}s_{12} - s_{13}c_{23}c_{12}e^{i\delta} & -s_{23}c_{12} - s_{13}c_{23}s_{12}e^{i\delta} & c_{13}c_{23} \end{pmatrix}, \quad (5)$$

where $c_{jk} \equiv \cos \theta_{jk}$ and $s_{jk} \equiv \sin \theta_{jk}$. In the most general U , the θ_{ij} are restricted to the first quadrant, $0 \leq \theta_{ij} \leq \pi/2$, with δ in the range $0 \leq \delta < 2\pi$. We assume that ν_3 is the neutrino eigenstate that is separated from the other two, and that the sign of δm_{31}^2 can be either positive or negative, corresponding to the case where ν_3 is either above or below, respectively, the other two mass eigenstates. The magnitude of δm_{31}^2 determines the oscillation length of atmospheric neutrinos, while the magnitude of δm_{21}^2 determines the oscillation length of solar neutrinos, and thus $|\delta m_{21}^2| \ll |\delta m_{31}^2|$. If we accept the likely conclusion that the solar solution is LMA [11], then $\delta m_{21}^2 > 0$ and we can restrict θ_{12} to the range $[0, \pi/4]$. It is known from reactor neutrino data that θ_{13} is small, with $\sin^2 2\theta_{13} \leq 0.1$ at the 95% C.L. [3]. Thus a set of parameters that unambiguously spans the space is δm_{31}^2 (magnitude and sign), δm_{21}^2 , $\sin^2 2\theta_{12}$, $\sin \theta_{23}$, and $\sin^2 2\theta_{13}$; only the θ_{23} angle can be below or above $\pi/4$.

In the context of three-neutrino models the usual method proposed for detecting CP violation in long-baseline experiments with a conventional neutrino beam is to measure the oscillation channels $\nu_\mu \rightarrow \nu_e$ and $\bar{\nu}_\mu \rightarrow \bar{\nu}_e$ (or $\nu_e \rightarrow \nu_\mu$ and $\bar{\nu}_e \rightarrow \bar{\nu}_\mu$ for a neutrino factory). Both leading and subleading oscillation contributions must be involved and the oscillations must be non-averaging for CP -violation effects [21]. For illustrative purposes we use the constant density matter approximation, although in an exact study variations of the density along the neutrino path should be implemented. Approximate formulas for the oscillation probabilities in matter of constant density in the limit $|\delta m_{21}^2| \ll A, |\delta m_{31}^2|$ already exist in the literature [17,18]. We adopt the form in Ref. [18], where θ_{13} is also treated as a small parameter and the mixing angles in matter are found in terms of an expansion in the small parameters θ_{13} and δm_{21}^2 . We introduce the notation

$$\Delta \equiv |\delta m_{31}^2|L/4E_\nu = 1.27|\delta m_{31}^2/\text{eV}^2|(L/\text{km})/(E_\nu/\text{GeV}), \quad (6)$$

$$\hat{A} \equiv |A/\delta m_{31}^2|, \quad (7)$$

$$\alpha \equiv |\delta m_{21}^2/\delta m_{31}^2|. \quad (8)$$

Up to second order in α and θ_{13} , the oscillation probabilities for $\delta m_{31}^2 > 0$ and $\delta m_{21}^2 > 0$ are

$$P(\nu_\mu \rightarrow \nu_e) = x^2 f^2 + 2xyfg(\cos \delta \cos \Delta - \sin \delta \sin \Delta) + y^2 g^2, \quad (9)$$

$$\bar{P}(\bar{\nu}_\mu \rightarrow \bar{\nu}_e) = x^2 \bar{f}^2 + 2xy\bar{f}g(\cos \delta \cos \Delta + \sin \delta \sin \Delta) + y^2 g^2, \quad (10)$$

respectively, where

$$x \equiv \sin \theta_{23} \sin 2\theta_{13}, \quad (11)$$

$$y \equiv \alpha \cos \theta_{23} \sin 2\theta_{12}, \quad (12)$$

$$f, \bar{f} \equiv \sin((1 \mp \hat{A})\Delta)/(1 \mp \hat{A}), \quad (13)$$

$$g \equiv \sin(\hat{A}\Delta)/\hat{A}. \quad (14)$$

The coefficients f and \bar{f} differ due to matter effects ($\hat{A} \neq 0$). To obtain the probabilities for $\delta m_{31}^2 < 0$, the transformations $\hat{A} \rightarrow -\hat{A}$, $y \rightarrow -y$ and $\Delta \rightarrow -\Delta$ (implying $f \leftrightarrow -\bar{f}$ and $g \rightarrow -g$) can be applied to the probabilities in Eqs. (9) and (10) to give

$$P(\nu_\mu \rightarrow \nu_e) = x^2 \bar{f}^2 - 2xy\bar{f}g(\cos \delta \cos \Delta + \sin \delta \sin \Delta) + y^2 g^2, \quad (15)$$

$$\bar{P}(\bar{\nu}_\mu \rightarrow \bar{\nu}_e) = x^2 f^2 - 2xyfg(\cos \delta \cos \Delta - \sin \delta \sin \Delta) + y^2 g^2. \quad (16)$$

For a T -reversed channel, the corresponding probabilities are found by changing the sign of the $\sin \delta$ term. In Eqs. (9), (10), (15), and (16) we have assumed $\delta m_{21}^2 > 0$, which is what one expects for the LMA solar solution; for $\delta m_{21}^2 < 0$, the corresponding formulae are obtained by $y \rightarrow -y$. These expressions are accurate as long as θ_{13} is not too large, and they are valid at $E_\nu > 0.5$ GeV ($\hat{A} \gtrsim 0.04(3 \times 10^{-3} \text{ eV}^2/|\delta m_{31}^2|)$) for all values of δm_{21}^2 currently favored by solar neutrino experiments. We expand on the domain of validity of these equations in the Appendix. The corresponding expansion in α and θ_{13} in a vacuum can be found by the substitutions $f, \bar{f}, g \rightarrow \sin \Delta$.

For reference, the conversion from \hat{A} and Δ to L and E_ν is shown in Fig. 1. For neutrinos with $\delta m_{31}^2 > 0$ or anti-neutrinos with $\delta m_{31}^2 < 0$, $\hat{A} = 1$ corresponds to an MSW resonance. For neutrinos, it can be shown that the choice $\hat{A} = 1/2$ maximizes both the $\sin \delta$ and $\cos \delta$ terms for a given Δ ; for anti-neutrinos the \hat{A} that maximizes the $\sin \delta$ and $\cos \delta$ terms varies with Δ .

We make two observations regarding the approximate probability formulas above, the consequences of which are discussed below:

- (i) Both terms that depend on the CP phase δ vanish when $g = 0$, i.e., at $\hat{A}\Delta = n\pi$, where n is an integer. The y^2 term also vanishes in this case, so that only the x^2 term survives.
- (ii) The $\cos \delta$ term vanishes when $\Delta = (n - \frac{1}{2})\pi$, while the $\sin \delta$ term vanishes when $\Delta = n\pi$.

The above statements are true for both neutrinos and anti-neutrinos.

The first observation implies that there is no sensitivity to the CP -violating phase δ when $\langle N_e \rangle L = \int N_e dL$ is an integer multiple of $\sqrt{2}\pi/G_F$, where $\langle N_e \rangle$ is the average value of N_e for the neutrino path. Numerically, for $n = 1$, this condition is

$$\langle N_e \rangle L \simeq 16275 \text{ km}, \quad (17)$$

or, for the Earth's density profile,

$$L \simeq 7600 \text{ km}. \quad (18)$$

This distance has a simple physical interpretation: it is the characteristic oscillation wavelength due to the matter interaction [19]. Furthermore, the condition in Eq. (17) is *independent of all oscillation parameters*. It is also independent of E_ν . It has often been noted that CP violation is strongly suppressed in long baseline experiments of order 7300 km (nominally the distance from Fermilab to Gran Sasso); we see that this is a universal effect that occurs because L is close to the oscillation length due to matter. Furthermore, the term proportional to y^2 also vanishes, which means that there is also no dependence on δm_{21}^2 or θ_{12}

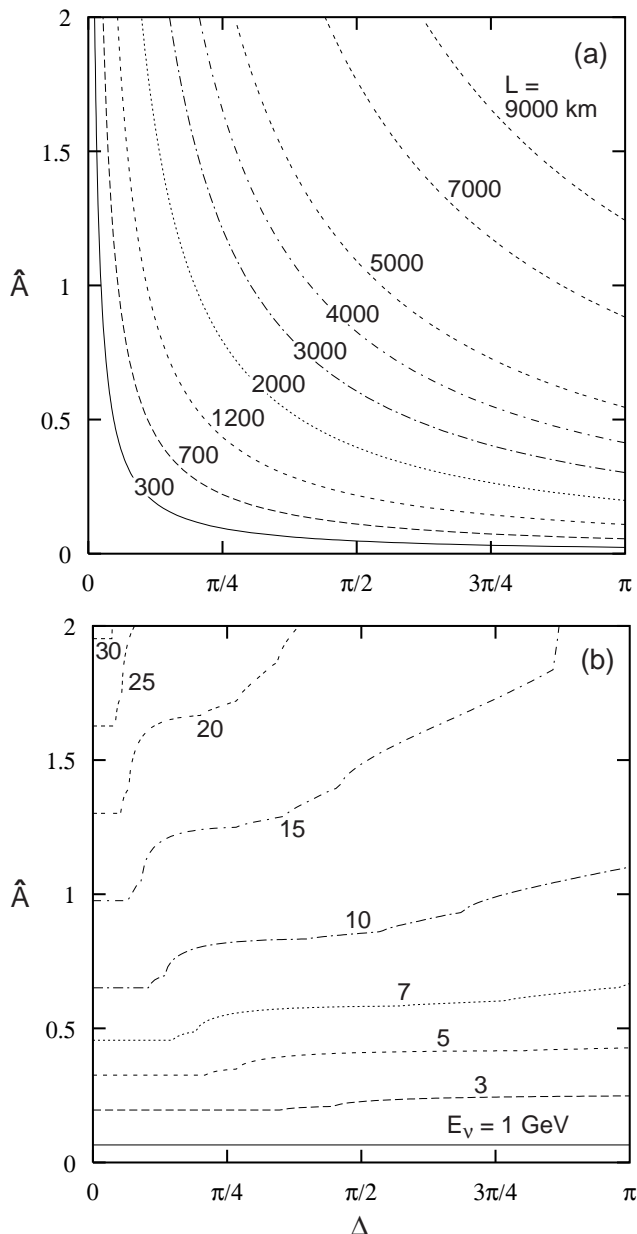


FIG. 1. Contours of (a) L and (b) E_ν versus \hat{A} and Δ , for $\delta m_{31}^2 = 3 \times 10^{-3} \text{ eV}^2$.

at this distance, at least to second order in the small parameters. Therefore this distance is especially well-suited for measuring θ_{13} without the complications of disentangling it from δ , θ_{12} , or δm_{21}^2 . For baselines greater than about 4000 km the constant density approximation loses accuracy (see results in the Appendix), so that the critical distance in Eq. (18) is not exact, but does explain semi-quantitatively the weakness of CP violating effects near that distance.

The second observation relates to the relative strength of the $\sin \delta$ and $\cos \delta$ terms in $P(\nu_\mu \rightarrow \nu_e)$. In short L , low E_ν experiments the matter effects are small and the leading terms of the oscillation probability are given by the vacuum formulas. Then L and E_ν

can be chosen such that only the explicitly CP -violating $\sin \delta$ term survives (e.g., when $\Delta = \pi/2$), and CP violation can be measured directly by comparing $P(\nu_\mu \rightarrow \nu_e)$ and $P(\bar{\nu}_\mu \rightarrow \bar{\nu}_e)$ (although even for $L \sim$ few 100 km there are small matter corrections that must be considered). However, as is evident from Eqs. (9) and (10), when θ_{13} is small the relative strengths of the $\sin \delta$ and $\cos \delta$ terms in the presence of large matter corrections at longer L can be selected by an appropriate choice of Δ *in exactly the same way* as in the short L , vacuum-like case. That is, the δ dependence with matter effects included can be made pure $\sin \delta$ for

$$L/E_\nu \simeq (2n - 1)(410 \text{ km/GeV}) \left(\frac{3 \times 10^{-3} \text{ eV}^2}{|\delta m_{31}^2|} \right), \quad (19)$$

where n is an integer *. The only caveat is that matter corrections are much larger for longer L and the accuracy of the determination of δ may be more subject to knowledge of the electron density.

B. Orbits in probability space

We assume that $\sin^2 2\theta_{23}$ and $|\delta m_{31}^2|$ are well-determined (perhaps at the few percent level or better) by a ν_μ survival or $\nu_\mu \rightarrow \nu_\tau$ measurement [8], and that θ_{12} and δm_{21}^2 are also well-determined (KamLAND should be able to measure the parameters of the solar LMA solution to the few percent level [12]). Then the remaining parameters to be determined are δ , θ_{13} , and the sign of δm_{31}^2 (the sign of δm_{21}^2 is positive for LMA).

The usual proposal for testing CP violation in the neutrino sector is to measure both $\nu_\mu \rightarrow \nu_e$ and $\bar{\nu}_\mu \rightarrow \bar{\nu}_e$ probabilities. As δ varies for given θ_{13} and $\text{sgn}(\delta m_{31}^2)$, an elliptical orbit will be traced in $P-\bar{P}$ space [16,22]. The shape of the ellipse is determined by the relative phases of the terms involving δ . We identify three possible cases:

- (i) $\Delta \neq n\pi/2$. In this case, both the $\sin \delta$ and $\cos \delta$ terms are nonzero and the orbit for fixed θ_{13} is an ellipse. Each value of δ gives a distinct point in $P-\bar{P}$ space for a given θ_{13} . For $\Delta = (n - \frac{1}{2})\frac{1}{2}\pi$ the ellipse has the maximum ‘‘fatness’’ [22], i.e., it is as close as possible to a circle given the values of f and \bar{f} .
- (ii) $\Delta = (n - \frac{1}{2})\pi$, where n is an integer. In this case the $\cos \delta$ term vanishes and the orbit ellipse collapses to a line. If $f \simeq \bar{f}$ (such as at short L where matter effects are small), CP violation is measured directly by comparing the ν and $\bar{\nu}$ event rates (after correcting for the differences in the cross sections and initial flux normalization).
- (iii) $\Delta = n\pi$. In this case the $\sin \delta$ term vanishes, the ellipse collapses to a line, and CP violation is measured indirectly by parametrically determining the value of δ and not by the measurement of a CP -violating quantity.

*The misconception that the $\cos \delta$ term dominates at large L and E_ν comes from extending the large E_ν approximation beyond its range of validity, as discussed in Ref. [18].

There will be two ellipses for each θ_{13} , one for each sign of δm_{31}^2 ; they both fall into the same class, i.e., if the ellipse for $\delta m_{31}^2 > 0$ is Case (ii), the ellipse for $\delta m_{31}^2 < 0$ will also be Case (ii).

C. CP degeneracy: (δ, θ_{13}) ambiguity

In many cases the parameters (δ, θ_{13}) can give the same probabilities as another pair of parameters (δ', θ'_{13}) , for fixed values of the other oscillation parameters; this is known as the “ (δ, θ_{13}) ambiguity” [23]. Using Eqs. (9) and (10), the general formulas for the parameters (x', δ') that give the same P and \bar{P} as (x, δ) for $\Delta \neq n\pi/2$ (Case (ii)) are

$$x' \cos \delta' = x \cos \delta + \frac{(f + \bar{f})(x^2 - x'^2)}{4yg \cos \Delta}, \quad (20)$$

$$x' \sin \delta' = x \sin \delta - \frac{(f - \bar{f})(x^2 - x'^2)}{4yg \sin \Delta}. \quad (21)$$

Equations (20) and (21) can be used to derive

$$x'^2 - x^2 = \frac{4yg \sin 2\Delta [yg \sin 2\Delta + xf \sin(\Delta - \delta) + x\bar{f} \sin(\Delta + \delta)]}{f^2 + \bar{f}^2 - 2f\bar{f} \cos 2\Delta}, \quad (22)$$

from which δ' can then be determined from Eq. (20) or (21). In particular, a set of parameters which violates CP ($\sin \delta' \neq 0$) can be degenerate with another set of parameters, with a different θ_{13} , that conserves CP ($\sin \delta = 0$). It can be shown that in all cases real solutions exist for x' , so there will be an ambiguity between two sets of oscillation parameters if $|\sin \delta'| \leq 1$. Therefore we conclude that the use of a monoenergetic beam at a fixed L will necessarily entail parameter ambiguities if only the channels $\nu_\mu \rightarrow \nu_e$ and $\bar{\nu}_\mu \rightarrow \bar{\nu}_e$ are measured. An example is shown in Fig. 2a for $\Delta = 3\pi/4$.

When $\Delta \neq n\pi/2$, the (δ, θ_{13}) ambiguity can give a degeneracy between CP violating (CPV) and CP conserving (CPC) solutions. If $\sin \delta = 0$ in Eq. (21), then $\sin \delta'$ is not zero if $f \neq \bar{f}$; the difference can be large if f and \bar{f} differ substantially due to large matter effects. For example, in Fig. 2a the prediction for (P, \bar{P}) for $(\sin^2 2\theta_{13}, \delta) = (0.01, 0)$ is identical to that for $(0.00298, 1.48\pi)$.

For the Cases (ii) and (iii) above, the ellipse collapses to a line. The ambiguities then reduce to $x' = x$ (see Eq. (22)) and $\sin \delta' = \sin \delta$ in Case (ii) and $\cos \delta' = \cos \delta$ in Case (iii). Thus the ambiguity no longer involves θ_{13} (and hence in principle θ_{13} is determined, at least as far as the (δ, θ_{13}) ambiguity is concerned), but instead is a $(\delta, \pi - \delta)$ ambiguity (which does not mix CPC and CPV solutions) in Case (ii) and a $(\delta, 2\pi - \delta)$ ambiguity in Case (iii). Examples for Cases (ii) and (iii) are shown in Figs. 2b and 2c, respectively. For $\Delta \simeq n\pi/2$ the orbit ellipse is very skinny and the ambiguous θ_{13} values are close to each other, which qualitatively is similar to either Case (ii) or Case (iii).

Note that in both Figs. 2b and 2c the orbit line has a negative slope. It can be shown that for $\hat{A} < 1$ (i.e., density less than the critical density for resonance) the orbit lines in (P, \bar{P}) space have negative slope for $\Delta = n\pi/2$. For $\hat{A} > 1$, the orbit lines for $\Delta = n\pi/2$ have positive slope.

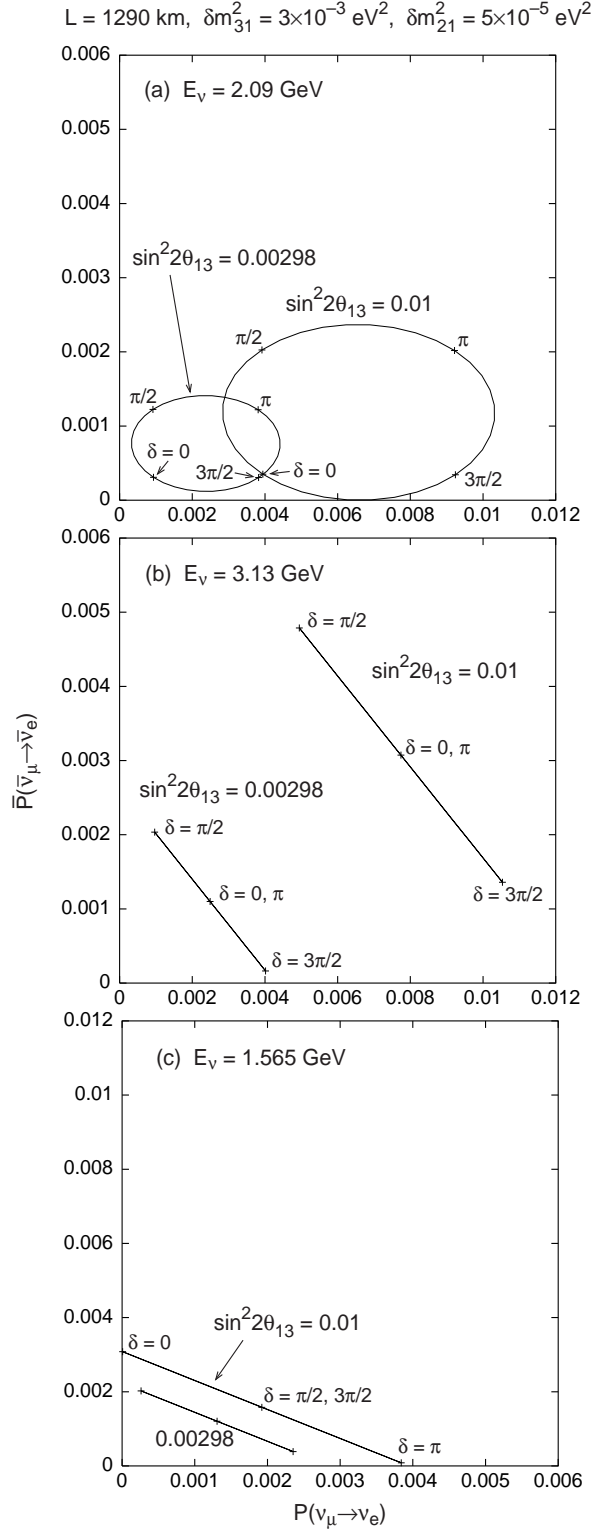


FIG. 2. Orbit ellipses showing (δ, θ_{13}) ambiguity for $L = 1290 \text{ km}$ with (a) $E_{\nu} = 2.09 \text{ GeV}$ ($\Delta = 3\pi/4$), (b) $E_{\nu} = 3.13 \text{ GeV}$ ($\Delta = \pi/2$), and (c) $E_{\nu} = 1.565 \text{ GeV}$ ($\Delta = \pi$), for $\sin^2 2\theta_{13} = 0.01$ and 0.00298 . The other parameters are $\delta m_{31}^2 = 3 \times 10^{-3} \text{ eV}^2$, $\delta m_{21}^2 = 5 \times 10^{-5} \text{ eV}^2$, $\sin^2 2\theta_{23} = 1$, and $\sin^2 2\theta_{12} = 0.8$. The value of δ varies around the ellipse. In (b) and (c) the ellipse collapses to a line and the ambiguity reduces to a $(\delta, \pi - \delta)$ or $(\delta, 2\pi - \delta)$ ambiguity, respectively, and different values of θ_{13} do not overlap (for the same $\text{sgn}(\delta m_{13}^2)$).

D. Mass hierarchy degeneracy: $\text{sgn}(\delta m_{31}^2)$ ambiguity

In addition to the (δ, θ_{13}) ambiguity discussed above for a given $\text{sgn}(\delta m_{31}^2)$, in some cases there are also parameters (δ', θ'_{13}) with $\delta m_{31}^2 < 0$ that give the same P and \bar{P} as (δ, θ_{13}) with $\delta m_{31}^2 > 0$. Three examples of the $\text{sgn}(\delta m_{31}^2)$ ambiguity are shown in Fig 3. Furthermore, there is also a (δ', θ'_{13}) ambiguity for $\delta m_{31}^2 < 0$, so in principle there can be a four-fold ambiguity, i.e., four sets of δ and θ_{13} (two for $\delta m_{31}^2 > 0$ and two for $\delta m_{31}^2 < 0$) that give the same P and \bar{P} .

As with the (δ, θ_{13}) ambiguity, the $\text{sgn}(\delta m_{31}^2)$ ambiguity can mix CP conserving and CP violating solutions. For example, in Fig. 3a the prediction for (P, \bar{P}) for $(\sin^2 2\theta_{13}, \delta) = (0.01, 0)$ with $\delta m_{31}^2 = 3 \times 10^{-3} \text{ eV}^2$ is identical to that for $(0.0138, 4\pi/3)$ with $\delta m_{31}^2 = -3 \times 10^{-3} \text{ eV}^2$.

Although the general equations for the $\text{sgn}(\delta m_{31}^2)$ ambiguity are somewhat messy, for the case $\Delta = (n - \frac{1}{2})\pi$ the values of (x', δ') for $\delta m_{31}^2 < 0$ that give the same P and \bar{P} as (x, δ) for $\delta m_{31}^2 > 0$ are determined by

$$x'^2 = \frac{x^2(f^2 + \bar{f}^2 - f\bar{f}) - 2yg(f - \bar{f})x \sin \delta \sin \Delta}{f\bar{f}}, \quad (23)$$

$$x' \sin \delta' = x \sin \delta \frac{f^2 + \bar{f}^2 - f\bar{f}}{f\bar{f}} - \frac{x^2}{\sin \Delta} \frac{f^2 + \bar{f}^2}{f\bar{f}} \frac{f - \bar{f}}{2yg}. \quad (24)$$

If $\sin \delta = 0$ then Eq. (24) reduces to

$$\sin \delta' = -x \frac{f^2 + \bar{f}^2}{f\bar{f}} \frac{f - \bar{f}}{2yg \sin \Delta} \sqrt{\frac{f\bar{f}}{f^2 + \bar{f}^2 - f\bar{f}}}, \quad (25)$$

which is not zero if $f \neq \bar{f}$, i.e., whenever there are matter effects, so there is a potential CPC/CPV confusion as long as the right-hand side of Eq. (25) has magnitude less than unity. It is possible to have $\delta' = \pi/2$ when $\delta = 0$, i.e., CPC can be confused with maximal CPV (see Fig. 3b).

The ambiguity between parameters with $\delta m_{31}^2 > 0$ and $\delta m_{31}^2 < 0$ occurs only for some values of δ , and does not occur at all if matter effects are large enough (i.e., L and θ_{13} are large enough) [24,25]. The conditions for the existence of this ambiguity will be discussed further in Sec. III B. Note, however, that the $\text{sgn}(\delta m_{31}^2)$ ambiguity can still confuse different values of δ and θ_{13} even for $\Delta = n\pi/2$ (see, e.g., Figs. 3b and 3c), unlike the (δ, θ_{13}) ambiguity where θ_{13} is removed from the ambiguity for $\Delta = n\pi/2$.

E. Atmospheric angle degeneracy: $(\theta_{23}, \pi/2 - \theta_{23})$ ambiguity

There is yet another ambiguity in the determination of δ and θ_{13} , which involves the value of θ_{23} . In practice it is only $\sin^2 2\theta_{23}$ that is determined by a ν_μ survival measurement (for now we ignore matter corrections to $\nu_\mu \rightarrow \nu_\mu$, which are relatively small for oscillations involving active flavors), so θ_{23} cannot be distinguished from $\pi/2 - \theta_{23}$. The effect of this degeneracy can be seen by interchanging $\sin \theta_{23}$ and $\cos \theta_{23}$ in Eqs. (11) and (12). For $\theta_{23} \simeq \pi/4$ (the favored solution from atmospheric data) the ambiguity vanishes, but for

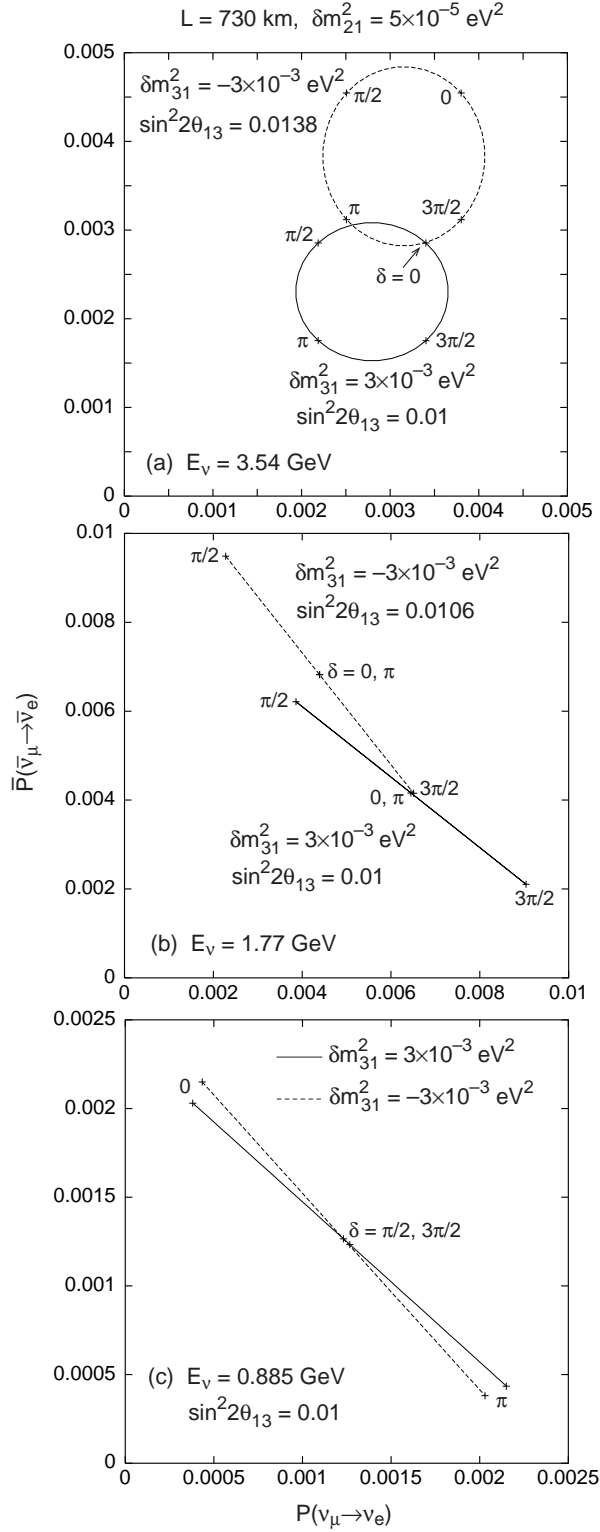


FIG. 3. $\text{Sgn}(\delta m_{31}^2)$ ambiguity for $L = 730 \text{ km}$ with (a) $E_\nu = 3.54 \text{ GeV}$ ($\Delta = \pi/4$), (b) $E_\nu = 1.77 \text{ GeV}$ ($\Delta = \pi/2$), and (c) $E_\nu = 0.885 \text{ GeV}$ ($\Delta = \pi$). The other parameters are $\delta m_{21}^2 = 5 \times 10^{-5} \text{ eV}^2$, $\sin^2 2\theta_{23} = 1$, and $\sin^2 2\theta_{12} = 0.8$.

$\sin^2 2\theta_{23} \simeq 0.9$ it can have a sizable effect, since in this case $\sin^2 \theta_{23} = 0.35$ and $\cos^2 \theta_{23} = 0.65$. Three examples of the θ_{23} ambiguity are shown in Fig. 4. The θ_{23} ambiguity can also mix *CPC* and *CPV* solutions; for example, in Fig. 4a, the prediction for (P, \bar{P}) for $(\sin^2 2\theta_{13}, \sin \theta_{23}, \delta) = (0.01, 0.585, 0)$ is identical to that for $(0.00107, 0.811, 4\pi/3)$.

As with the $\text{sgn}(\delta m_{31}^2)$ ambiguity, the equations for the θ_{23} ambiguity are rather messy in the general case. For the special case $\Delta = (n - \frac{1}{2})\pi$, we have

$$\sin^2 2\theta'_{13} = \sin^2 2\theta_{13} \tan^2 \theta_{23} + \frac{\alpha^2 g^2 \sin^2 2\theta_{12}}{f\bar{f}} (1 - \tan^2 \theta_{23}), \quad (26)$$

$$\sin 2\theta'_{13} \sin \delta' = \sin 2\theta_{13} \sin \delta + \frac{\alpha g(f - \bar{f}) \sin 2\theta_{12} \cot 2\theta_{23}}{f\bar{f} \sin \Delta}, \quad (27)$$

where (δ, θ_{13}) are the parameters that give a certain (P, \bar{P}) for $0 < \theta_{23} < \pi/4$ and (δ', θ'_{13}) are the parameters that give the same (P, \bar{P}) for $\pi/2 - \theta_{23}$. We see that even for $\Delta = n\pi/2$ the θ_{23} ambiguity can mix *CPC* and *CPV* solutions, since $\sin \delta = 0$ does not necessarily imply $\sin \delta' = 0$. Furthermore, even for $\Delta = n\pi/2$ the θ_{23} ambiguity mixes solutions with different θ_{13} (see Eqs. (26) and (27), and Figs. 4b and 4c), unlike the (δ, θ_{13}) ambiguity where θ_{13} is removed from the ambiguity for $\Delta = n\pi/2$.

Since α is a small parameter (and possibly even small compared to $\sin 2\theta_{13}$), the numerical uncertainty in δ due to the θ_{23} ambiguity is generally small, of order 0.07π or less, when $\Delta = (n - \frac{1}{2})\pi$, $L = 2900$ km, $\delta m_{21}^2 = 10^{-4}$ eV², and $\sin^2 2\theta_{13} = 0.01$. This effect is of order the expected experimental uncertainty in δ [16,26]. The size of the δ ambiguity decreases with decreasing matter effect (smaller L) and with decreasing δm_{21}^2 , so for a wide range of parameters the *CPC/CPV* confusion from the θ_{23} ambiguity is not too severe. On the other hand, the $\sin^2 2\theta_{13}$ confusion is approximately a factor $\tan^2 \theta_{23}$ (see Eq. (26)), which lies roughly in the range $\frac{1}{2}$ to 2 for $\sin^2 2\theta_{23} \geq 0.9$.

F. Comments on parameter degeneracies

In the preceding three sections we have shown that in principle there can be as much as an eight-fold ambiguity in determining δ and θ_{13} from $P(\nu_\mu \rightarrow \nu_e)$ and $\bar{P}(\bar{\nu}_\mu \rightarrow \bar{\nu}_e)$ at a single L and E_ν , which comes from the presence of three independent two-fold ambiguities: (δ, θ_{13}) , $\text{sgn}(\delta m_{31}^2)$, and $(\theta_{23}, \pi/2 - \theta_{23})$. For each type of ambiguity there is the possibility of being unable to distinguish between *CP* violating and *CP* conserving parameters. Measurements at multiple L and E_ν can be used to help discriminate the different degenerate solutions, but that would involve extra detectors or a much longer total running time, and probably reduced statistics for each (L, E_ν) combination. In the next section we will explore what L and E_ν values do best at resolving these potential degeneracies without resorting to measurements at different L and/or E_ν . We then will examine what L and E_ν for a second measurement can remove the remaining degeneracies.

In the Appendix we demonstrate that the analytic expressions are accurate for $E_\nu > 0.5$ GeV for baselines up to 4000-5000 km. For much lower E_ν (as low as 0.05 GeV) they are still accurate at shorter distances ($L \lesssim 350$ km) if α and θ_{13} are not too large (see the discussion in the Appendix). Therefore we expect that the qualitative aspects of the three ambiguities are unchanged for short L , low E_ν experiments such as CERN-Frejus.

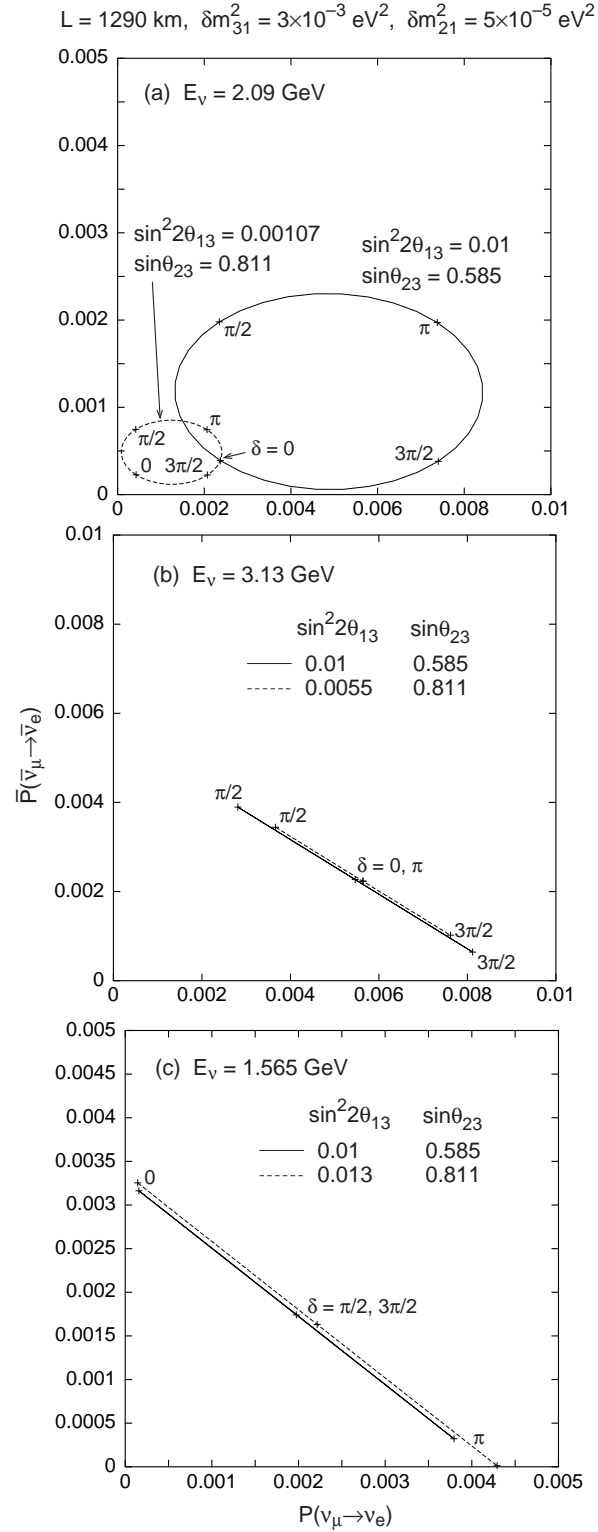


FIG. 4. $(\theta_{23}, \pi/2 - \theta_{23})$ ambiguity for $L = 1290 \text{ km}$ with (a) $E_\nu = 2.09 \text{ GeV}$ ($\Delta = 3\pi/4$), (b) $E_\nu = 3.13 \text{ GeV}$ ($\Delta = \pi/2$), and (c) $E_\nu = 1.565 \text{ GeV}$ ($\Delta = \pi$). The other parameters are $\delta m_{21}^2 = 5 \times 10^{-5} \text{ eV}^2$, and $\sin^2 2\theta_{12} = 0.8$.

TABLE II. Possible neutrino beam energies E_ν (in GeV) versus baseline (in km) and Δ that will convert the (δ, θ_{13}) ambiguity to a simple $(\delta, \pi - \delta)$ ambiguity, for $\delta m_{31}^2 = 3 \times 10^{-3} \text{ eV}^2$. For other values of δm_{31}^2 , E_ν scales proportionately with δm_{31}^2 . Only values of $E_\nu > 0.5 \text{ GeV}$ are considered.

Δ	300 km	730 km	1290 km	1770 km	2100 km	2600 km	2900 km
$\frac{\pi}{2}$	0.73	1.77	3.13	4.29	5.12	6.34	7.03
$\frac{3\pi}{2}$		0.59	1.04	1.43	1.71	2.11	2.34
$\frac{5\pi}{2}$			0.63	0.86	1.02	1.27	1.41
$\frac{7\pi}{2}$				0.61	0.73	0.91	1.00
$\frac{9\pi}{2}$					0.57	0.70	0.78

III. RESOLVING PARAMETER DEGENERACIES

A. Resolving the (δ, θ_{13}) ambiguity

As discussed in Secs. IIB and IIC, the choice $\Delta = n\pi/2$ causes the orbit ellipse in (P, \bar{P}) space to collapse to a line and the (δ, θ_{13}) ambiguity reduces to one involving only δ , i.e., the combination of P and \bar{P} gives a unique value of θ_{13} (at least for one sign of δm_{31}^2). Furthermore, since δ only becomes confused with $\pi - \delta$ (in Case (ii) of Sec. IIC) or $2\pi - \delta$ (in Case (iii)), CP conserving solutions never become mixed with CP violating ones. Case (ii) (with $\Delta = (n - \frac{1}{2})\pi$) has another advantage in that the $\nu_\mu \rightarrow \nu_\tau$ oscillation is approximately maximal (see Eq. (A3)), which would facilitate a better measurement of $\sin^2 2\theta_{23}$ and δm_{31}^2 . Therefore the choice $\Delta = (n - \frac{1}{2})\pi$ is the best for resolving the (δ, θ_{13}) ambiguity. Some representative beam energies for particular baselines are given in Table II.

B. Resolving the $\text{sgn}(\delta m_{31}^2)$ ambiguity

The parameter degeneracy associated with the sign of δm_{31}^2 can be overcome if there is a large matter effect that splits P and \bar{P} , e.g., if L is sufficiently long and θ_{13} is not too small [24,25]. To determine the minimum value of θ_{13} that avoids the $\text{sgn}(\delta m_{31}^2)$ ambiguity, we must first find the region in (P, \bar{P}) space covered by each $\text{sgn}(\delta m_{31}^2)$, and then determine the condition on θ_{13} that ensures the regions for different $\text{sgn}(\delta m_{31}^2)$ do not overlap.

The orbit ellipse for a given $\text{sgn}(\delta m_{31}^2)$ moves as θ_{13} changes, sweeping out a region in (P, \bar{P}) space. All points on each orbit ellipse (for a given θ_{13}) that lie inside the region will overlap an orbit ellipse for a different θ_{13} (this is what leads to the (δ, θ_{13}) ambiguity). However, the points on the orbit ellipse that lie on the boundaries of the region do not have a (δ, θ_{13}) ambiguity, i.e., there are unique values of θ_{13} and δ for that point. This implies that for points on the boundary of the region, $x = x'$ and $\delta = \delta'$ in Eqs. (20)–(22). For $\Delta \neq n\pi/2$, the condition becomes $xf \sin(\Delta - \delta) + x\bar{f} \sin(\Delta + \delta) + yg \sin 2\Delta = 0$. Solving for δ and substituting into Eqs. (9) and (10) we find the coordinates of the $\delta m_{31}^2 > 0$ envelope in (P, \bar{P}) space are given by

$$P = x^2 f^2 + y^2 g^2 - \frac{2y^2 g^2 f^2 \sin^2 2\Delta \pm 2ygf\sqrt{z}(f \cos 2\Delta - \bar{f})}{f^2 + \bar{f}^2 - 2ff \cos 2\Delta}, \quad (28)$$

where

$$z = x^2(f^2 + \bar{f}^2 - 2f\bar{f}\cos 2\Delta) - y^2g^2\sin^2 2\Delta, \quad (29)$$

and \bar{P} is found by interchanging $f \leftrightarrow \bar{f}$ and letting $g \rightarrow -g$. For $\delta m_{31}^2 < 0$, the values of P and \bar{P} on the envelope can be found by interchanging P and \bar{P} . Although the general solution is complicated, for the special case $\Delta = (n - \frac{1}{2})\pi$ it is not hard to show that the two $\text{sgn}(\delta m_{31}^2)$ regions do not overlap if

$$x > \frac{2yg}{f - \bar{f}}. \quad (30)$$

Note that matter effects split f and \bar{f} , which decreases the minimum value of value of x (and hence of $\sin^2 2\theta_{13}$) needed to avoid any $\text{sgn}(\delta m_{31}^2)$ ambiguity. Because $x \propto \sin 2\theta_{13}$ and $y \propto \delta m_{21}^2$, the corresponding minimum value of $\sin^2 2\theta_{13}$ increases as the square of δm_{21}^2 . The minimum values of $\sin^2 2\theta_{13}/(\delta m_{21}^2)^2$ are plotted versus E_ν for various values of L in Fig. 5. For $\Delta = \pi/2$, the $\text{sgn}(\delta m_{31}^2)$ ambiguity would be resolved for $\sin^2 2\theta_{13} > 0.01$ (0.04) at $L = 1290$ km, the distance from Fermilab to Homestake, if $\delta m_{21}^2 = 5 \times 10^{-5}$ (10^{-4}) eV^2 . For $L \simeq 2600$ km (Brookhaven–Homestake or Fermilab–San Jacinto), $\text{sgn}(\delta m_{31}^2)$ can be determined for values of $\sin^2 2\theta_{13}$ as low as 0.002 (0.008) for $\delta m_{21}^2 = 5 \times 10^{-5}$ (10^{-4}) eV^2 .

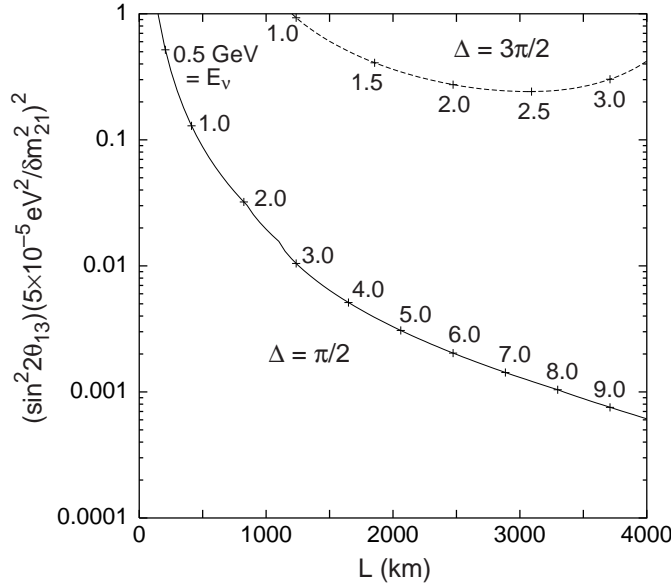


FIG. 5. Minimum value of $\sin^2 2\theta_{13}/(\delta m_{21}^2)^2$ that avoids the $\text{sgn}(\delta m_{31}^2)$ ambiguity, plotted versus L for $\Delta = \pi/2$ (solid curve) and $3\pi/2$ (dashed), with $\delta m_{31}^2 = 3 \times 10^{-3}$ eV^2 . The corresponding values of E_ν are marked on the curves.

Figure 5 shows that $\Delta = 3\pi/2$ would be unsatisfactory in distinguishing $\text{sgn}(\delta m_{31}^2)$; in fact, measurements at $\Delta = (n - \frac{1}{2})\pi$ do increasingly worse as n increases, as can be shown using Eq. (13). For $\Delta = (n - \frac{1}{2})\pi$, we have $|f/\bar{f}| = (1 + \hat{A})/(1 - \hat{A})$; since \hat{A} is proportional to E_ν , and E_ν decreases with n for fixed L , larger values of n will have smaller \hat{A} . Thus, the values of f and \bar{f} will be closer for larger n , reducing the size of the matter effect (at least as far as splitting P and \bar{P} is concerned). For $\Delta = 3\pi/2$ and

$\delta m_{32}^2 = 5 \times 10^{-5} \text{ eV}^2$, the value of $\sin^2 2\theta_{13}$ must be greater than about 0.25 which is excluded by CHOOZ [3]. Even the most optimistic case for $\Delta = 3\pi/2$ (which occurs for the highest value of $\delta m_{21}^2 (\simeq 10^{-4} \text{ eV}^2)$ allowed in the LMA region) requires $\sin^2 2\theta_{13} \gtrsim 0.06$. Thus, the proposal of Ref. [27] to perform experiments at higher n suffers from an inability to determine $\text{sgn}(\delta m_{31}^2)$. Practically speaking, only $n = 1$ will provide sufficient discrimination for $\text{sgn}(\delta m_{31}^2)$ if Δ is restricted to the values $(n - \frac{1}{2})\pi$. We henceforth restrict ourselves to this case.

By combining $\Delta = \pi/2$ with a sufficiently long L , the combined four-fold ambiguity involving δ , θ_{13} , and $\text{sgn}(\delta m_{31}^2)$ can be reduced to a simple $(\delta, \pi - \delta)$ ambiguity that in principle determines whether CP is conserved or violated. Some possibilities are shown in Figs. 6 and 7. As Fig. 6 shows, for $\delta m_{21}^2 = 5 \times 10^{-5} \text{ eV}^2$, $L = 1290 \text{ km}$ is (barely) sufficient to distinguish $\text{sgn}(\delta m_{31}^2)$ for $\sin^2 2\theta_{13}$ as low as 0.01. However, for $\delta m_{21}^2 = 10^{-4} \text{ eV}^2$, $L > 2000 \text{ km}$ is needed. In practice, experimental uncertainties and uncertainties on the matter distribution [28] increase the likelihood of having a $\text{sgn}(\delta m_{31}^2)$ ambiguity, so that a separation of the two regions greater than the size of the experimental uncertainties is required.

C. Resolving the $(\theta_{23}, \pi/2 - \theta_{23})$ ambiguity

Even if Δ is chosen to mitigate the effects of the (δ, θ_{13}) ambiguity, and L is chosen long enough to eliminate the $\text{sgn}(\delta m_{31}^2)$ ambiguity, there still remains the $(\theta_{23}, \pi/2 - \theta_{23})$ ambiguity. If $\theta_{23} \simeq \pi/4$ this ambiguity disappears, and choosing L and E_ν such that $\Delta = \pi/2$ leaves a simple $(\delta, \pi - \delta)$ ambiguity. If θ_{23} deviates from $\pi/4$, then there does not appear to be a judicious choice of a single L and E_ν that can resolve the θ_{23} ambiguity.

The problem in resolving the θ_{23} ambiguity lies in the fact that in the leading term in $P(\nu_\mu \rightarrow \nu_e)$ and $\bar{P}(\bar{\nu}_\mu \rightarrow \bar{\nu}_e)$, $\sin 2\theta_{13}$ is always paired with $\sin \theta_{23}$ (see Eqs. (9) and (10)), and so if there are two values of θ_{23} derived from the measured value of $\sin^2 2\theta_{23}$, there will be two corresponding values of $\sin^2 2\theta_{13}$. Since $\sin^2 2\theta_{23}$ can be as low as 0.9, the two values of $\sin^2 \theta_{23}$ can be as far apart as 0.35 and 0.65, and therefore the ambiguity in $\sin^2 2\theta_{13}$ can be as large as a factor 1.86 at leading order (Eq. (26) in the limit that α is small). The next-to-leading term in the probabilities in Eqs. (9) and (10) is proportional to $\sin 2\theta_{23}$, and therefore cannot resolve the ambiguity. The last term in $P(\nu_\mu \rightarrow \nu_e)$ is proportional to $\cos^2 \theta_{23}$, so that the relative weighting of the last term compared to the leading term is affected by the value of $\sin \theta_{23}$. However, the last term is suppressed by α^2 , and is generally much smaller than the leading term (at least for $\sin^2 2\theta_{13} \geq 0.01$, the approximate region where superbeam experiments will be able to probe). Hence, even measurements at a second L and E_ν would likely be unable to resolve the θ_{23} ambiguity if it exists (i.e., θ_{23} not close to $\pi/4$).

If one could also measure $P(\nu_e \rightarrow \nu_\tau)$ (see Appendix A for an approximate analytic expression), then a comparison with $P(\nu_e \rightarrow \nu_\mu)$ should determine whether θ_{23} is above or below $\pi/4$; the leading term in $P(\nu_e \rightarrow \nu_\tau)$ can be obtained from the leading term in $P(\nu_\mu \rightarrow \nu_e)$ by the replacement of $\sin \theta_{23}$ by $\cos \theta_{23}$. A $\nu_e \rightarrow \nu_\tau$ measurement could be done in a neutrino factory; in fact, a neutrino factory may be the only practical way to resolve the θ_{23} ambiguity, if it exists. A neutrino factory experiment also provides energy spectrum information that could be helpful in resolving parameter ambiguities [23,29].

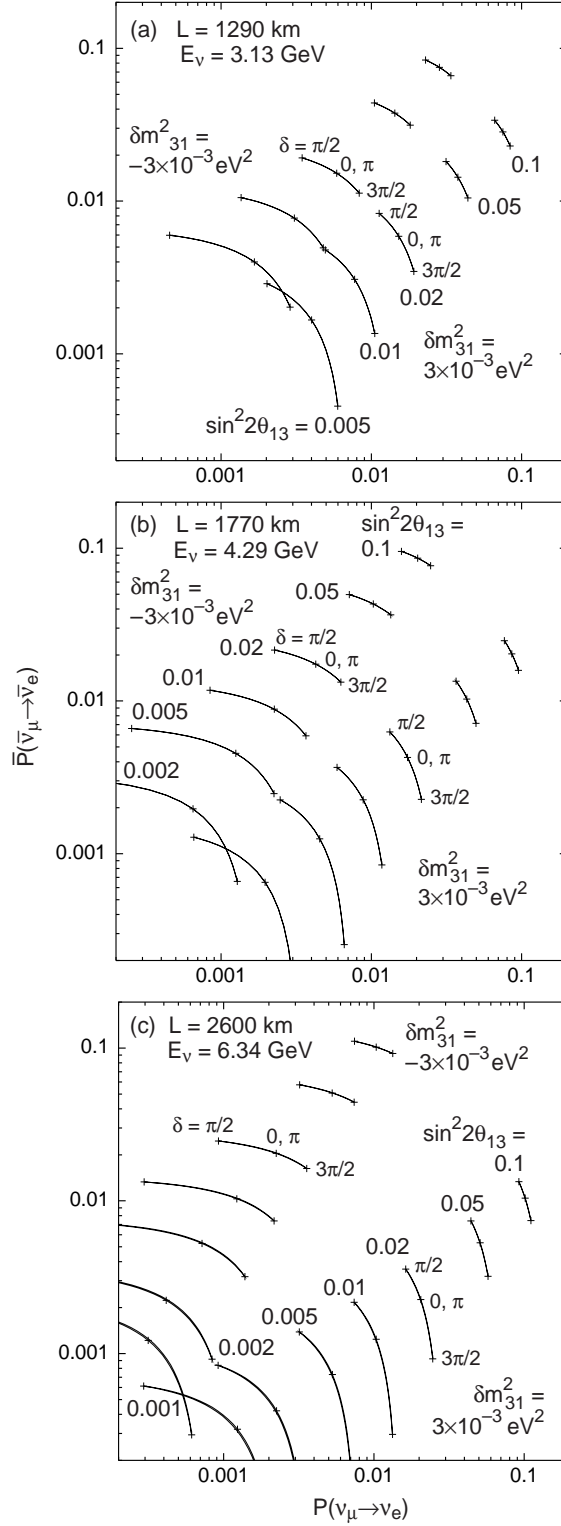


FIG. 6. Resolution of combined (δ, θ_{13}) and $\text{sgn}(\delta m_{31}^2)$ ambiguities when $\Delta = \pi/2$, for (a) $L = 1290$ km, (b) $L = 1770$ km, and (c) $L = 2900$ km, with $|\delta m_{31}^2| = 3 \times 10^{-3} \text{ eV}^2$, $|\delta m_{21}^2| = 5 \times 10^{-5} \text{ eV}^2$, and $\sin^2 2\theta_{23} = 1$.

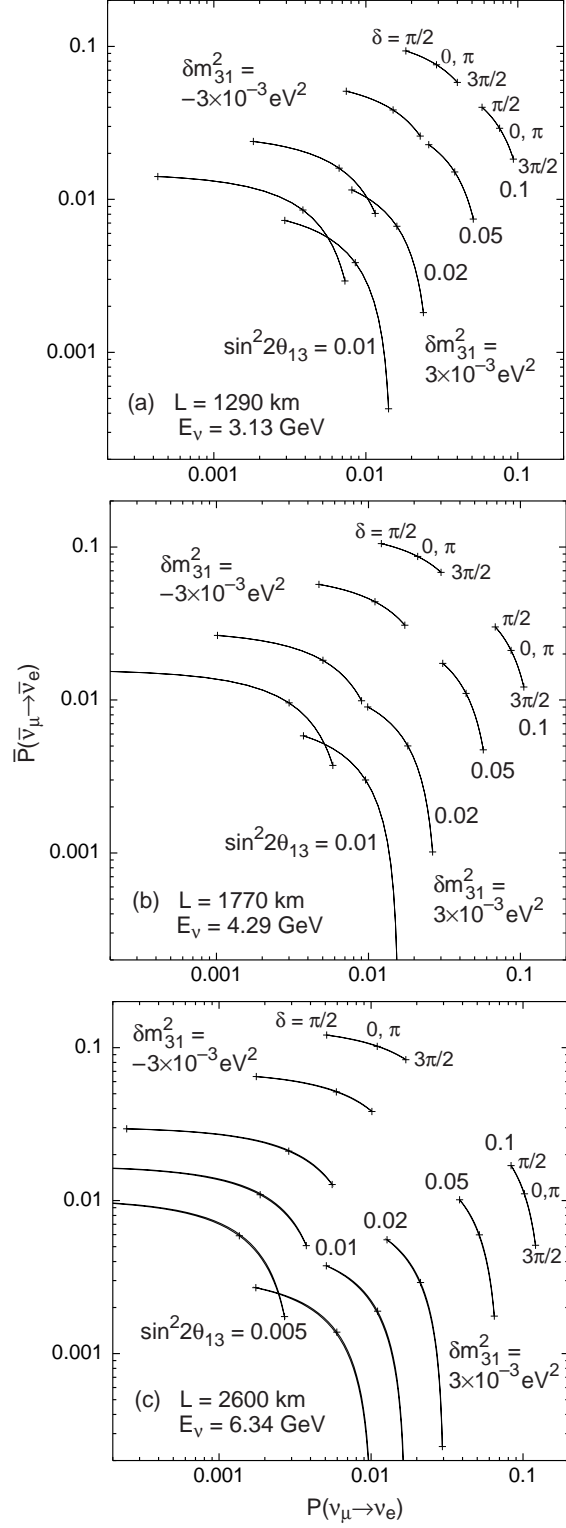


FIG. 7. Same as Fig. 6, except for $|\delta m_{21}^2| = 10^{-4} \text{ eV}^2$.

D. Measurements at a second L and/or E_ν

As we have demonstrated, measurements at a single L and E_ν cannot resolve all parameter ambiguities. A second experiment at a different L and/or E_ν , with a different value of Δ , is required for this purpose. The best sets of L and E_ν are those that are complementary, i.e., the second experiment should provide the clearest distinction between the parameter ambiguities of the first experiment. In this section we discuss three possible scenarios, each with measurements at two L and E_ν combinations.

1. Scenario A

In this scenario, the first measurement would be done at $\Delta_1 = \pi/2$ (with L/E_ν given by Eq. (19)). As discussed earlier, this choice isolates the $\sin \delta$ term, removes θ_{13} from the (δ, θ_{13}) ambiguity, and the remaining $(\delta, \pi - \delta)$ ambiguity does not mix CPC and CPV solutions. These L/E_ν values also give a large ν_μ disappearance, which facilitates the precision measurement of δm_{31}^2 and $\sin^2 2\theta_{23}$. The baseline L should be large enough to avoid the $\text{sgn}(\delta m_{31}^2)$ ambiguity ($L \gtrsim 2000$ km assures this for $\sin^2 2\theta_{13} \gtrsim 0.01$). Representative values of L and E_ν are given in Table II. Measuring $P(\nu_\mu \rightarrow \nu_e)$ and $\bar{P}(\bar{\nu}_\mu \rightarrow \bar{\nu}_e)$ at one such L and E_ν should determine $\text{sgn}(\delta m_{31}^2)$, θ_{13} (modulo the θ_{23} ambiguity, if present), and whether or not CP is violated (as discussed in Sec. II E, the existence of a θ_{23} ambiguity will not give a large amount of CPC/CPV confusion).

The second measurement should be one that best resolves the $(\delta, \pi - \delta)$ ambiguity. In principle, $\Delta_2 = \pi$, which eliminates the $\sin \delta$ terms in the probabilities and leaves only $\cos \delta$ terms, gives the maximal separation of δ and $\pi - \delta$. Thus, the first measurement gives $\sin \delta$, the second gives $\cos \delta$, from which the value of δ may be inferred. Furthermore, if θ_{13} is determined from the first measurement, then both P and \bar{P} would not have to be measured in the second measurement; one is sufficient to determine δ . Whether one used neutrinos or antineutrinos in the second measurement would be determined by which gave the larger event rate, taking into account neutrino fluxes, cross sections, and oscillation probabilities. If $\delta m_{31}^2 > 0$, then neutrinos would be best for the second measurement, due to the larger flux and cross section; for $\delta m_{31}^2 < 0$, antineutrinos may be the better choice if the matter enhancement is enough to overcome the lower flux and cross section for antineutrinos. If both the first and second measurements are done at the same L , then $\Delta_2 = \pi$ means that the appropriate energy in the second experiment is $E_2 = E_1/2$.

In practice, there are other values Δ_2 that are not close to $\pi/2$ that could potentially work for the second measurement. The optimal Δ_2 also depends on the particular values of f , \bar{f} and g at the various L and E_ν , as well as on neutrino parameters that are currently unknown (δm_{21}^2 , θ_{12} , and θ_{13}). We do not pursue the optimization here.

2. Scenario B

If the first measurement is done at an L that is not large enough to resolve the $\text{sgn}(\delta m_{31}^2)$ ambiguity, then the second measurement must be tailored to both determine $\text{sgn}(\delta m_{31}^2)$ and resolve the $(\delta, \pi - \delta)$ ambiguity, i.e., it must break a four-fold degeneracy. As discussed

TABLE III. Possible sets of neutrino beam energies and baselines that will resolve the four-fold parameter ambiguity when the measurements are done at shorter L (such that the $\text{sgn}(\delta m_{31}^2)$ ambiguity is not resolved in either experiment).

Fixed L (km)	E_1 (GeV)	E_2 (GeV)
300	0.73	0.355, 0.375
730	1.77	0.835, 0.940
Fixed E (GeV)	L_1 (km)	L_2 (km)
0.73	300	575, 630
1.77	730	1295, 1700

above, the choice $\Delta_2 = \pi$ determines δ , but it can be shown that at shorter L an approximate degeneracy with parameters of the opposite $\text{sgn}(\delta m_{31}^2)$ remains (e.g., see Fig. 3c). Another example is shown in Fig. 8a, where the near degeneracy of parameters with the opposite $\text{sgn}(\delta m_{31}^2)$ remains for some values of δ (while the crosses in Fig. 8a are well-separated in the second measurement, the boxes are not). However, at $\Delta_2 = \pi/(1 \pm \hat{A})$, either \bar{f} or f vanishes (depending on the sign of δm_{31}^2), and the four ambiguous solutions occupy four separate regions in (P, \bar{P}) space, as shown in Fig. 8b. Although the four regions in Fig. 8b overlap somewhat, when the point of one degenerate solution is in the overlap region the points of the other three degenerate solutions are not (the crosses and boxes are always well-separated). Thus the four-fold ambiguity involving $(\delta, \pi - \delta)$ and $\text{sgn}(\delta m_{31}^2)$ will always be resolved. A disadvantage of Scenario B is that because either f or \bar{f} is zero in the second measurement, P and \bar{P} tend to be smaller, so that event rates may be somewhat lower than for other values of Δ .

Some examples are given in Table III. For instance, if the first baseline is $L_1 = 730$ km (Fermilab to Soudan), then $\Delta_1 = \pi/2$ for $E = 1.77$ GeV, and two possibilities for a second experiment with the same beam energy are $L_2 = 1295$ and 1700 km, which serendipitously are very close to the distances from Fermilab to Homestake and from Fermilab to Carlsbad (or Brookhaven to Soudan).

In practice, narrow band beams are not monoenergetic. However, values of Δ_2 close to $\pi/(1 \pm \hat{A})$ also give reasonably good separation of the ambiguities, as long as Δ_2 is not close to π . If the fractional beam spread is more than $|\hat{A}|$, a slightly different average value of Δ_2 might be preferable, to ensure that no significant part of the beam has Δ_2 too close to π .

Fig. 9 summarizes the possibilities for Scenarios A and B, showing E_ν versus L for the first measurement done at $\Delta_1 = \pi/2$ (solid curve) and a possible second measurement at $\Delta_2 = \pi$ (Scenario A, dotted curve) or $\pi/(1 \pm \hat{A})$ (Scenario B, dashed curves).

3. Scenario C

This scenario uses the fact that the probabilities are insensitive to the parameters of the δm_{21}^2 scale at $L \simeq 7600$ km, as noted in Sec. II B. If the first measurement of P and \bar{P} were done at $L \simeq 7600$ km, θ_{13} would be determined (modulo the θ_{23} ambiguity), and because the distance is large enough $\text{sgn}(\delta m_{31}^2)$ would also be determined from the large matter effect. A second measurement of P and \bar{P} could then be done at an L and E_ν such that $\Delta = (2n - 1)\pi/4$, which gives the maximum “fatness” of the orbit ellipse [22] (see Sec. II B), which in turn should best distinguish different values of δ . One disadvantage of

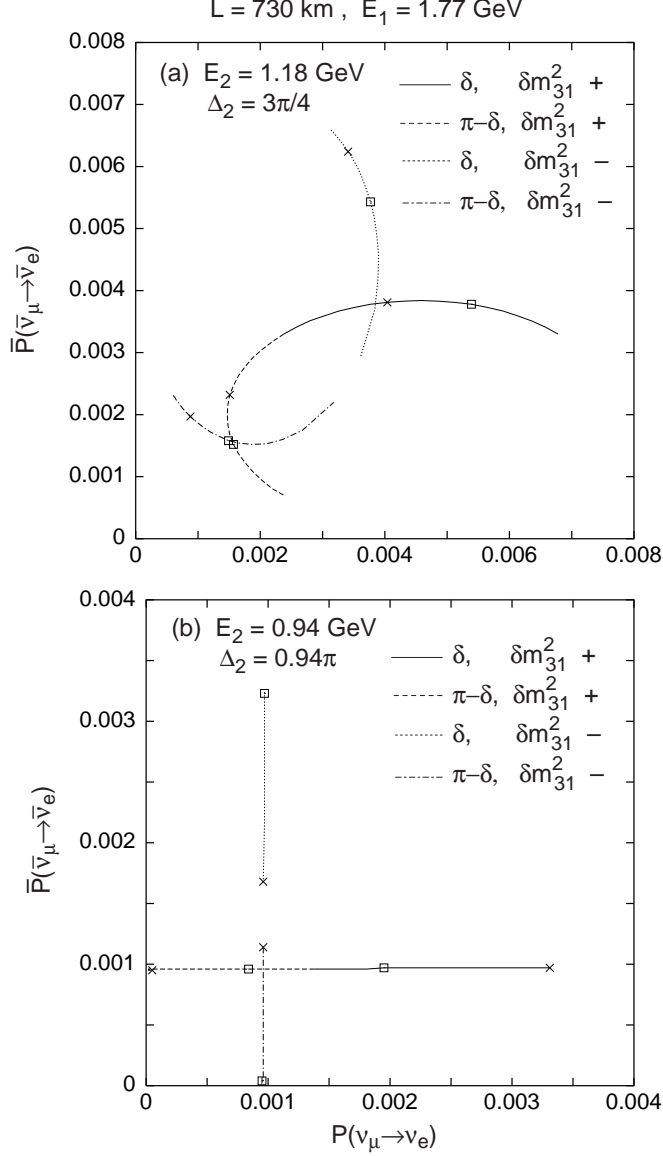


FIG. 8. Values of P and \bar{P} in a second measurement when there is a four-fold degeneracy in the first measurement for (a) $E_2 = 1.18 \text{ GeV}$ ($\Delta_2 = 3\pi/4$) and (b) $E_2 = 0.94 \text{ GeV}$ ($\Delta_2 = \pi/(1 + \hat{A}) = 0.94\pi$), with $L_1 = L_2 = 730 \text{ km}$ and $E_1 = 1.77 \text{ GeV}$ ($\Delta_1 = \pi/2$). Each curve (solid, dashed, dotted, dash-dotted) represents one of the four solutions that are degenerate. Points labelled by the same symbol (crosses or boxes) correspond to solutions that are degenerate with each other in the measurement at L_1 and E_1 .

Scenarios B and C compared to Scenario A is that both P and \bar{P} must be determined in both measurements.

4. Discussion of scenarios

Although the three scenarios discussed above are not necessarily the only solutions to the ambiguities, in each case one measurement is chosen to eliminate one or more of the

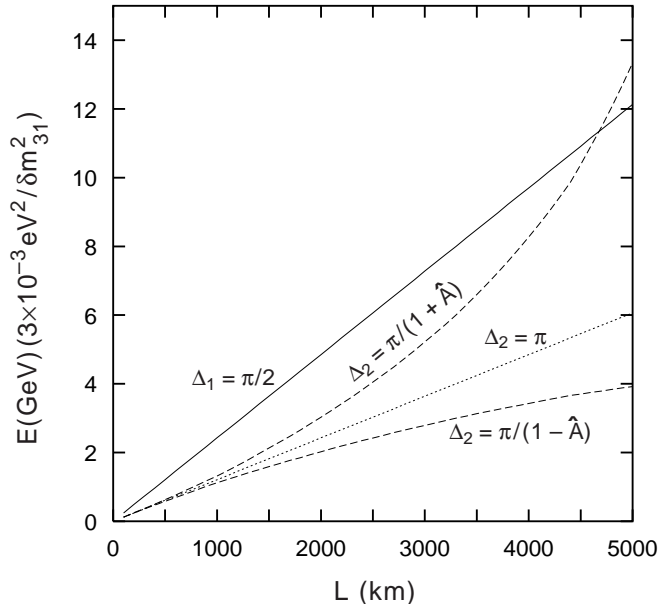


FIG. 9. Values of L and E_ν for a first measurement at $\Delta_1 = \pi/2$ (solid curve) and a second measurement at $\Delta_2 = \pi$ (Scenario A, dotted) or $\pi/(1 \pm \hat{A})$ (Scenario B, dashed), which breaks the parameter degeneracy in each case.

parameters from the ambiguities, leaving the second measurement to resolve only the remaining ambiguities. In this sense, they are cleaner measurements. Scenario A would appear to be more favorable, since in principle the first measurement alone could determine $\sin \delta$, $\text{sgn}(\delta m_{31}^2)$, and θ_{13} (modulo the θ_{23} ambiguity), and thus determine whether or not CP is violated. Also, as discussed in Sec. II E, even if there is a θ_{23} ambiguity, the magnitude of the CPC/CPV confusion appears to be relatively small for the usual range of neutrino parameters considered.

5. Implication for JHF experiments

The proposed SuperJHF–HyperKamiokande experiment [16] satisfies the requirements for the first experiment of Scenario B. The plan is to have a neutrino energy such that Δ is at the first peak of the oscillation for $L = 300$ km; if Δ is not exactly on the peak (e.g., if $\delta m_{31}^2 = 3 \times 10^{-3} \text{ eV}^2$), a long narrow ellipse results instead of a straight line (see Fig. 10). Because the distance is relatively short, the $\text{sgn}(\delta m_{31}^2)$ ambiguity is not likely to be resolved since there is considerable overlap of the two $\text{sgn}(\delta m_{31}^2)$ ellipses (see Fig. 10b). For example, for $\sin^2 2\theta_{13} = 0.01$ the point for $\delta = 0$ with $\delta m_{31}^2 > 0$ is nearly the same as the point for $\delta = 1.18\pi$ for $\delta m_{31}^2 < 0$ (Eq. 25, which measures the size of the CPC/CPV confusion for the $\text{sgn}(\delta m_{31}^2)$ ambiguity, gives the about the same numerical result). The expected 90% C.L. uncertainty in δ in this case is about 0.07π near $\delta = 0$ [16], so we see that the $\text{sgn}(\delta m_{31}^2)$ ambiguity caused by the matter effect would seriously impede a proper measurement of δ , although there is the possibility that the SuperJHF–HyperK experiment might measure a point (P, \bar{P}) that was sufficiently outside the overlap region,

thereby determining $\text{sgn}(\delta m_{31}^2)$ [22]. A possible $(\theta_{23}, \pi/2 - \theta_{23})$ ambiguity also remains, which could lead to a corresponding ambiguity in θ_{13} , as shown in Fig. 10c.

Even though JHF may not sit exactly on the peak of the oscillation (i.e., $\Delta = \pi/2$), Fig. 10 shows that the three ambiguities discussed here are present. Also, Fig. 10a shows that the ambiguity in θ_{13} is relatively small (of order 10% or less) if Δ is close, but not exactly equal, to $\pi/2$. Thus as long as L/E_ν is chosen so that the oscillation is close to the first peak, we expect that the scenarios discussed here for determining the neutrino mass and mixing parameters will be valid.

IV. SUMMARY

There is an eight-fold, (δ, θ_{13}) - $\text{sgn}(\delta m_{31}^2)$ - $(\theta_{23}, \pi/2 - \theta_{23})$ degeneracy affecting the neutrino mixing matrix determined in long-baseline neutrino oscillation experiments. If $\sin^2 2\theta_{23}$ is almost unity as is favored by current Super-K and K2K data, this is reduced to a four-fold ambiguity. To break this four-fold ambiguity to a simple $(\delta, \pi - \delta)$ ambiguity which does not interfere with a determination of whether or not CP is violated in the neutrino sector, we find that an experiment should be performed at the first oscillation maximum corresponding to $\Delta = \pi/2$ and at a baseline of at least about 1300–2000 km, depending on the value of δm_{21}^2 . Representative values of L and E_ν that yield $\Delta = \pi/2$ are given in Table II.

The obvious advantages of choosing $\Delta = \pi/2$ are that $\nu_\mu \rightarrow \nu_e$ transitions are nearly maximal even when matter effects are accounted for and the $\nu_\mu \rightarrow \nu_\tau$ oscillation (which has small matter effects) is maximal, allowing a precise measurement of $\sin^2 2\theta_{23}$ and δm_{31}^2 . By choosing $\Delta = \pi/2$, the (δ, θ_{13}) degeneracy represented by the P - \bar{P} ellipse collapses to a line leaving a $(\delta, \pi - \delta)$ ambiguity (see Fig. 2) which unambiguously determines whether or not CP is violated. The central reason for the choice of the first oscillation peak over other peaks is that practically speaking, the $\text{sgn}(\delta m_{31}^2)$ ambiguity can be resolved only for this peak (see Fig. 5). The other peaks succeed in eliminating this ambiguity only for the smallest values of δm_{21}^2 in the LMA region and for $\sin^2 2\theta_{13}$ close to the CHOOZ bound. As shown in Figs. 6-7 to remove this ambiguity simultaneously with the (δ, θ_{13}) ambiguity requires that the baseline be at least 1300 km for $\sin^2 2\theta_{13} > 0.01$ and $\delta m_{21}^2 = 5 \times 10^{-5} \text{ eV}^2$. For lower values of $\sin^2 2\theta_{13}$ and/or higher values of δm_{21}^2 , longer baselines than this are needed. The exciting aspect of an experiment at $\Delta = \pi/2$ and a sufficiently long baseline is that all degeneracies other than the $(\theta_{23}, \pi/2 - \theta_{23})$ degeneracy can be broken to a harmless $(\delta, \pi - \delta)$ ambiguity with only a single baseline and energy. The remaining $(\delta, \pi - \delta)$ ambiguity can be removed by making a second measurement at $\Delta = \pi$ which leaves only $\cos \delta$ terms in the probabilities and provides the maximal separation between δ and $\pi - \delta$. The $(\theta_{23}, \pi/2 - \theta_{23})$ degeneracy cannot be eliminated even with measurements at a second baseline and energy because in the leading term in $P(\nu_\mu \rightarrow \nu_e)$ and $\bar{P}(\bar{\nu}_\mu \rightarrow \bar{\nu}_e)$, $\sin 2\theta_{13}$ is paired with $\sin \theta_{23}$ (see Eqs. (9) and (10)). Fortunately, the mixing of the CPC and CPV solutions arising from this degeneracy are of order or smaller than the experimental uncertainty in δ , thereby making it less severe. Only a neutrino factory, which offers the unique ability to compare $P(\nu_e \rightarrow \nu_\mu)$ and $P(\nu_e \rightarrow \nu_\tau)$, can disentangle $\sin 2\theta_{13}$ from $\sin \theta_{23}$ and find whether θ_{23} is less than or greater than $\pi/4$.

If it is not possible to have an experiment with L sufficiently large to find $\text{sgn}(\delta m_{31}^2)$, a second experiment is necessary to simultaneously resolve the $(\delta, \pi - \delta)$ ambiguity and

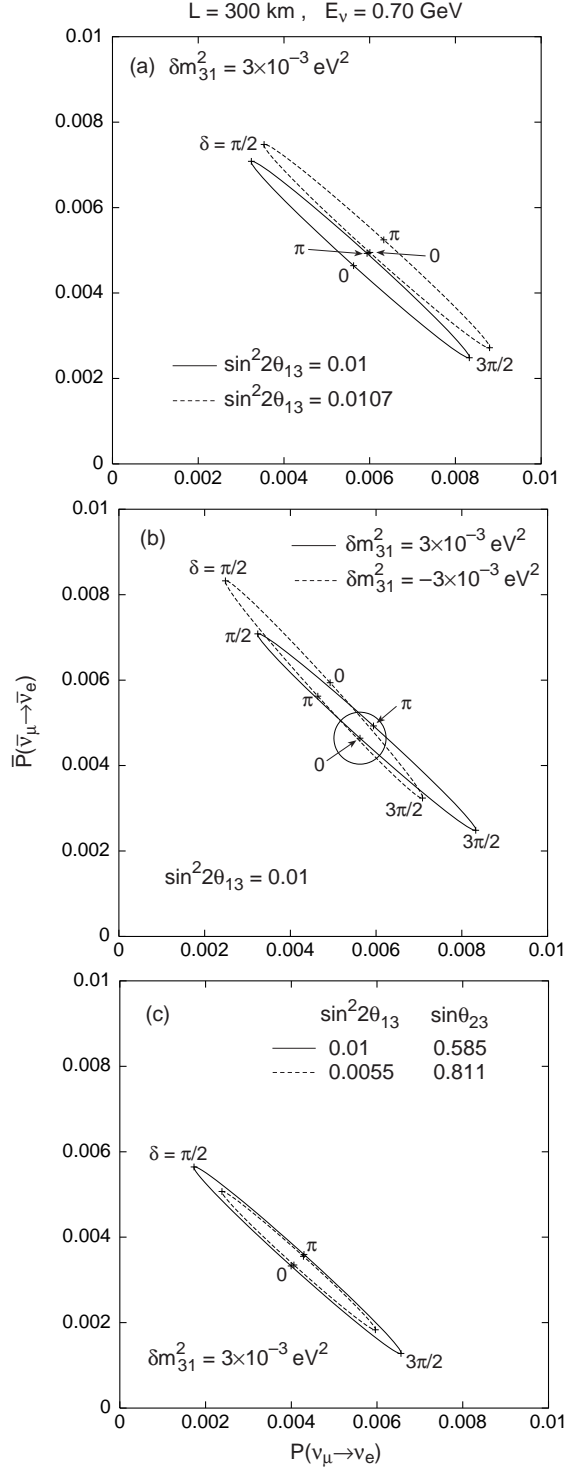


FIG. 10. Examples of the three types of ambiguities for the proposed SuperJHF–HyperK experiment [16] with $L = 300 \text{ km}$ and $E_\nu = 0.7 \text{ GeV}$: (a) (δ, θ_{13}) ambiguity, (b) $\text{sgn}(\delta m_{31}^2)$ ambiguity, and (c) $(\theta_{23}, \pi/2 - \theta_{23})$ ambiguity. In each case $\delta m_{21}^2 = 5 \times 10^{-5} \text{ eV}^2$, $\sin^2 2\theta_{23} = 1$, and $\sin^2 2\theta_{12} = 0.8$, unless otherwise stated in the figure. The circle in (b) indicates the size of the expected experimental uncertainties [16].

determine $\text{sgn}(\delta m_{31}^2)$. One possibility is to chose $\Delta = \pi$, but as suggested by Fig. 3c, a $\text{sgn}(\delta m_{31}^2)$ ambiguity may still remain when experimental errors are included. If $\Delta = \pi/(1 \pm \hat{A})$, either f or \bar{f} vanishes, depending on $\text{sgn}(\delta m_{31}^2)$, and the four-fold degeneracy breaks into four separate regions as in Fig. 8b. See Table III for some examples of how this scenario can be implemented. The proposed SuperJHF–HyperK experiment would satisfy the requirements for the first measurement of this type; it has the limitation of a possible $\text{sgn}(\delta m_{31}^2)$ confusion that leads to an ambiguity in the value of δ , which may compromise its ability to unambiguously establish CP violation.

In Fig. 9 we summarize the baselines and energies for two measurements, one at $\Delta_1 = \pi/2$ and another at either $\Delta_2 = \pi$ (if the first measurement can determine $\text{sgn}(\delta m_{31}^2)$ and only the $(\delta, \pi - \delta)$ ambiguity needs resolution) or $\Delta_2 = \pi/(1 \pm \hat{A})$ (if the first measurement can not be performed at a long enough baseline and the four-fold degeneracy $(\delta, \pi - \delta)$ - $\text{sgn}(\delta m_{31}^2)$ needs to be broken). Another possibility is to have one measurement at $L \simeq 7600$ km with $\hat{A}\Delta_1 = \pi$ and a second measurement with $\Delta_2 \simeq (2n - 1)\pi/4$. If K2K, MINOS, ICARUS and OPERA find that θ_{23} is not very close to $\pi/4$, a neutrino factory will be needed to resolve the $(\theta_{23}, \pi/2 - \theta_{23})$ ambiguity.

In our analysis we have assumed that δm_{31}^2 and $\sin^2 2\theta_{23}$ are known when the experiments described here are done. In fact, they will likely be determined only to 10% or so. Once these uncertainties are included the minimum value of L required to resolve the $\text{sgn}(\delta m_{31}^2)$ ambiguity, e.g., in Scenario A, could be slightly longer than indicated here. Also, because δm_{31}^2 is not precisely known, the average neutrino energy will not necessarily be exactly at the peak defined by $\Delta = \pi/2$. However, as our analysis of the proposed SuperJHF–HyperK experiment shows, only minimal uncertainties in δ and $\sin^2 2\theta_{13}$ are introduced by these factors, and the three principal ambiguities discussed in this paper will be qualitatively unchanged.

ACKNOWLEDGMENTS

This research was supported in part by the U.S. Department of Energy under Grants No. DE-FG02-95ER40896, No. DE-FG02-01ER41155 and No. DE-FG02-91ER40676, and in part by the University of Wisconsin Research Committee with funds granted by the Wisconsin Alumni Research Foundation.

APPENDIX A:

We provide a complete set of analytic expressions for the off-diagonal probabilities that are valid in the regime $|\hat{A}| > |\alpha|$, which roughly translates to $E_\nu > 0.5$ GeV. The diagonal probabilities can easily be found from them. The off-diagonal probabilities are for a normal hierarchy (in addition to Eqs. (9) and (10))

$$P(\nu_e \rightarrow \nu_\tau) = \cot^2 \theta_{23} x^2 f^2 - 2xyfg(\cos \delta \cos \Delta + \sin \delta \sin \Delta) + \tan^2 \theta_{23} y^2 g^2, \quad (\text{A1})$$

$$\bar{P}(\bar{\nu}_e \rightarrow \bar{\nu}_\tau) = \cot^2 \theta_{23} x^2 \bar{f}^2 - 2xy\bar{f}g(\cos \delta \cos \Delta - \sin \delta \sin \Delta) + \tan^2 \theta_{23} y^2 g^2, \quad (\text{A2})$$

and

$$P(\nu_\mu \rightarrow \nu_\tau) = \sin^2 2\theta_{23} \sin^2 \Delta + \alpha \sin 2\theta_{23} \sin 2\Delta \left(\frac{\hat{A}}{1 - \hat{A}} \sin \theta_{13} \sin 2\theta_{12} \cos 2\theta_{23} \sin \Delta - \Delta \cos^2 \theta_{12} \sin 2\theta_{23} \right). \quad (\text{A3})$$

For $\bar{P}(\bar{\nu}_\mu \rightarrow \bar{\nu}_\tau)$, replace \hat{A} by $-\hat{A}$ in Eq. (A3). Note that $P(\nu_\mu \rightarrow \nu_\tau)$ is independent of δ to $\mathcal{O}(\alpha)$. To obtain the probabilities for an inverted hierarchy, the transformations $\hat{A} \rightarrow -\hat{A}$, $\alpha \rightarrow -\alpha$ and $\Delta \rightarrow -\Delta$ must be made (implying $f \leftrightarrow -\bar{f}$ and $g \rightarrow -g$ in Eqs. (A1-A2), and for the T -reversed channels the sign of the $\sin \delta$ term must be changed.

We now compare the results of the analytic expressions with the numerical integration of the evolution equations of neutrinos through the Earth. We integrate the equations along a neutrino path using a Runge-Kutta method. The step size at each point along the path is 0.1% of the shortest oscillation wavelength given by the scales δm_{31}^2 and A . We account for the dependence of the density on depth by using the Preliminary Reference Earth Model (PREM) [30]. To calculate the analytic probability, we use the average value of the electron density along the neutrino path. We provide some values in Table IV for the reader's use; they are not indicative of the precision with which the electron density is known. We include subleading θ_{13} effects, which however are not relevant for $\sin^2 2\theta_{13}$ of $\mathcal{O}(0.01)$ or smaller. They are of importance at θ_{13} for which the CHOOZ limit $\sin^2 2\theta_{13} < 0.1$ (at 95% C. L.) is saturated. The parameters chosen to make this comparison are $\delta m_{31}^2 = 3.5 \times 10^{-3}$ eV², $\delta m_{21}^2 = 5 \times 10^{-5}$ eV², $\theta_{23} = \pi/4$, $\theta_{12} = \pi/6$, $\sin^2 2\theta_{13} = 0.01$ and $E_\nu = 5$ GeV. Thus, the ensuing comparison is not affected by dropping subleading θ_{13} effects. A normal mass hierarchy ($\delta m_{31}^2 > 0$) is assumed. We will comment on the comparison involving an inverted mass hierarchy.

Figure 11 shows $P(\nu_\mu \rightarrow \nu_e)$ and $P(\bar{\nu}_\mu \rightarrow \bar{\nu}_e)$ versus distance for $\delta = 0, \pi/2, \pi$, and $7\pi/4$. The agreement between the analytic formulae (solid lines) and the numerical results (dashed lines) is excellent for distances up to about 4000 km. Beyond that, the overlap between the lines degrades and for $L \gtrsim 5000$ km, the analytic equation completely breaks down. The analytic expression for $P(\bar{\nu}_\mu \rightarrow \bar{\nu}_e)$ works for much longer distances than that for $P(\nu_\mu \rightarrow \nu_e)$. Analogously, for the inverted mass hierarchy, $P(\nu_\mu \rightarrow \nu_e)$ is valid to longer distances than $P(\bar{\nu}_\mu \rightarrow \bar{\nu}_e)$.

Reference [18] claims good agreement between the analytic and numerical results for L even larger than 10000 km when a constant density is assumed for the Earth's density profile. The use of a realistic density profile as in the PREM model shows that the agreement deteriorates at much smaller distances.

For the sake of completeness we display the corresponding comparisons for $P(\nu_e \rightarrow \nu_\tau)$, $\bar{P}(\bar{\nu}_e \rightarrow \bar{\nu}_\tau)$ and $P(\nu_\mu \rightarrow \nu_\tau)$ in Figs. 12 and 13. The parameter values chosen are the same as for Fig. 11. The range of validity of Eqs. (A1) and (A2) is the same as for Eqs. (9) and (10). However, Eq. (A3) agrees almost exactly with the numerical result for the entire range considered. This is because matter effects are very small in comparison to the leading contribution. For the same reason, $\bar{P}(\bar{\nu}_\mu \rightarrow \bar{\nu}_\tau)$ is almost identical to $P(\nu_\mu \rightarrow \nu_\tau)$.

In Fig. 14, we show how well the analytic probabilities $P(\nu_\mu \rightarrow \nu_e)$ and $\bar{P}(\bar{\nu}_\mu \rightarrow \bar{\nu}_e)$ agree with the numerical integration for $L = 2900$ km (the longest baseline emphasized in this work) as a function of neutrino energy. The oscillation parameters used are the same as for Fig. 11. The precision is remarkable for the spectrum of energies of interest. For shorter baselines, the agreement gets even better.

We now make some cautionary remarks. Our comparisons were made for $\alpha = 0.0143$, the parameter in which the series was expanded, and $\sin^2 2\theta_{13} = 0.01$ which is assumed to be no greater than of $\mathcal{O}(\alpha)$. These values are motivated by the existing reactor bounds and global fits to the atmospheric and solar data. However, as either of these parameters gets larger, the agreement between the analytic equations and the numerical results deteriorates at long baselines even if subleading θ_{13} effects are included. Conversely, the agreement improves with smaller values of α and θ_{13} . As a rule of thumb, we recommend that the constant density approximation to the probabilities be used only for distances less than 4000 km. As can be seen from Fig. 15, for $L < 4000$ km, the density profile is nearly constant for most of the neutrino path, thereby satisfying the implicit assumption (of a constant density profile) under which analytic probabilities are valid.

We have stated that the analytic expressions are accurate for $E_\nu > 0.5$ GeV for baselines of 4000-5000 km. This robust bound can be relaxed for $L \lesssim 350$ km to E_ν as low as 0.05 GeV. However, for such low values of E_ν , the sensitivity of the analytic probabilities to α and θ_{13} is high and care must be taken in their use. For example, a comparison with a numerical integration is desirable if α and θ_{13} are relatively large.

Baseline (km)	$\langle N_e \rangle$
0 – 800	1.284400
900	1.320264
1000	1.356722
1100	1.374506
1200	1.474359
1300	1.516450
1400	1.543904
1500	1.563676
1600	1.578441
1700	1.590218
1800	1.599484
1900	1.607012
2000	1.613276
2100	1.618752
2200	1.622966
2300	1.626689
2400	1.630101
2500	1.633021
2600	1.635155
2700	1.636799
2800	1.638902
2900	1.640515
3000	1.641341
3100	1.642923
3200	1.643719
3300	1.644499
3400	1.653481
3500	1.659367
3600	1.663974
3700	1.668762
3800	1.672956
3900	1.676851
4000	1.681093

TABLE IV. The average values of the electron density $\langle N_e \rangle$ at baselines for which the analytic approximations of the probabilities accurately represent the numerical integration of the evolution equations.

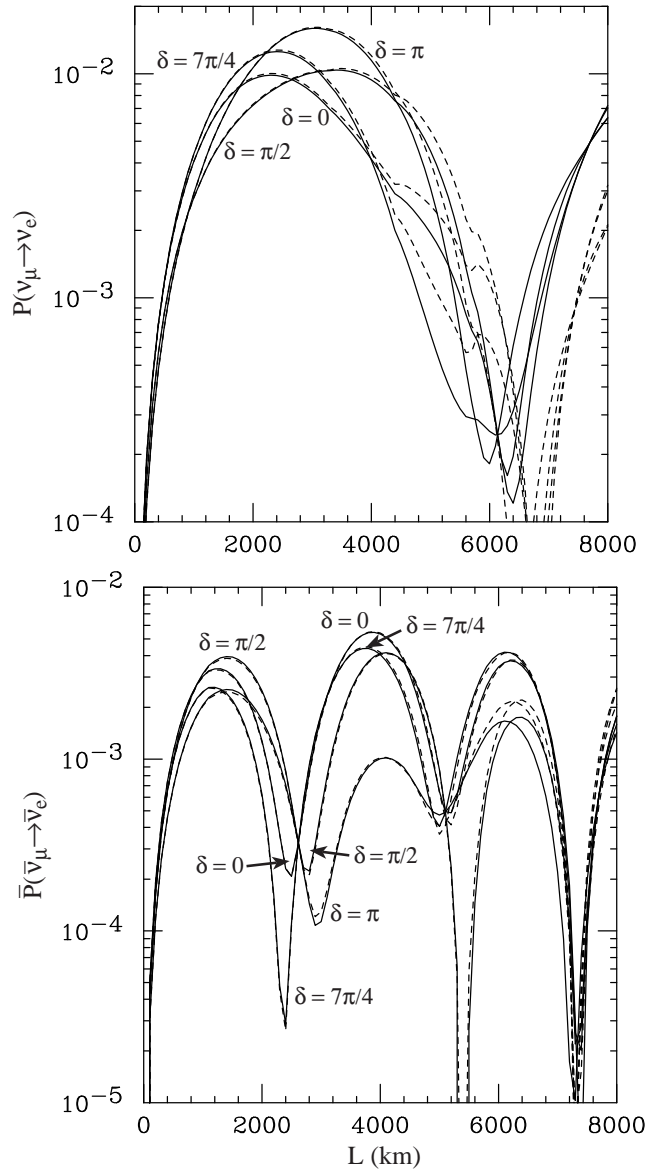


FIG. 11. $P(\nu_\mu \rightarrow \nu_e)$ and $\bar{P}(\bar{\nu}_\mu \rightarrow \bar{\nu}_e)$ versus L for $\delta = 0, \pi/2, \pi, 7\pi/4$. The agreement between the analytic formulae (solid lines) and the numerical results (dashed lines) is excellent for distances up to about 4000 km. The parameters chosen to make this comparison are $\delta m_{31}^2 = 3.5 \times 10^{-3} \text{eV}^2$, $\delta m_{21}^2 = 5 \times 10^{-5} \text{eV}^2$, $\theta_{23} = \pi/4$, $\theta_{12} = \pi/6$, $\sin^2 2\theta_{13} = 0.01$ and $E_\nu = 5 \text{ GeV}$.

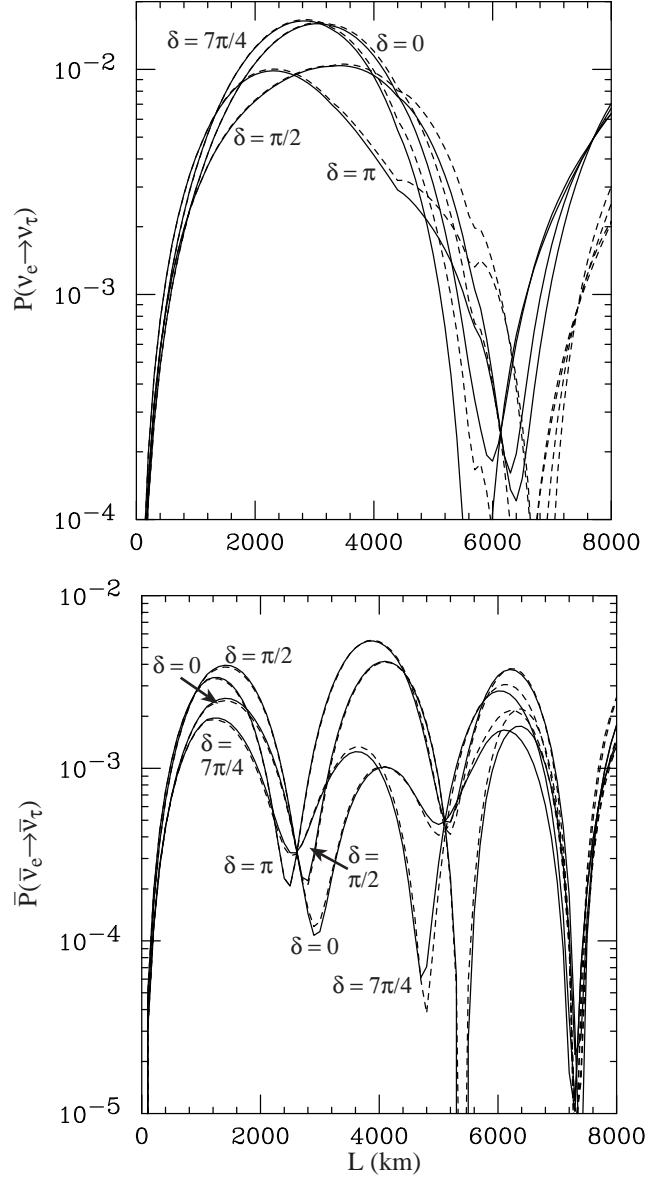


FIG. 12. $P(\nu_e \rightarrow \nu_\tau)$ and $\bar{P}(\bar{\nu}_e \rightarrow \bar{\nu}_\tau)$ versus L for the same set of parameters as in Fig. 11.

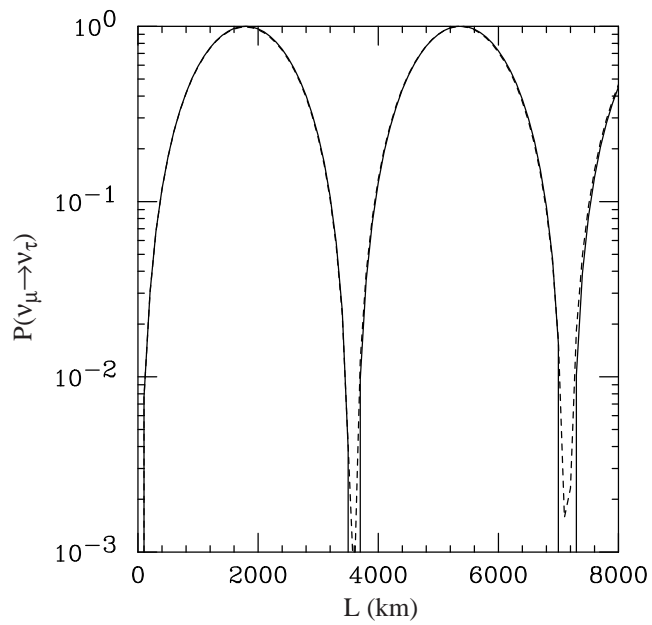


FIG. 13. $P(\nu_\mu \rightarrow \nu_\tau)$ versus L . The analytic expression (solid line) and the numerical calculation (dashed line) agree almost exactly for the entire range in L . $\bar{P}(\bar{\nu}_\mu \rightarrow \bar{\nu}_\tau)$ is almost identical to $P(\nu_\mu \rightarrow \nu_\tau)$ because of insignificant matter effects.

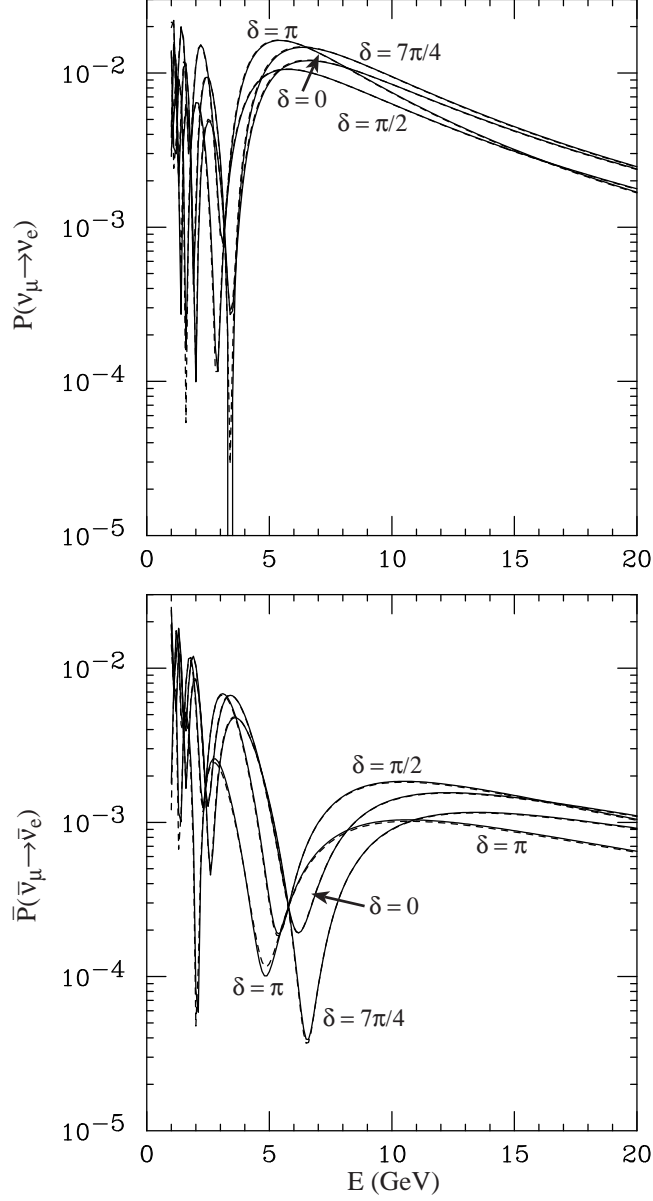


FIG. 14. $P(\nu_\mu \rightarrow \nu_e)$ and $\bar{P}(\bar{\nu}_\mu \rightarrow \bar{\nu}_e)$ vs E_ν for $L = 2900$ km. The oscillation parameters are the same as in Fig. 11. The solid lines (analytic equations) and dashed lines (numerical evaluation) are almost undistinguishable.

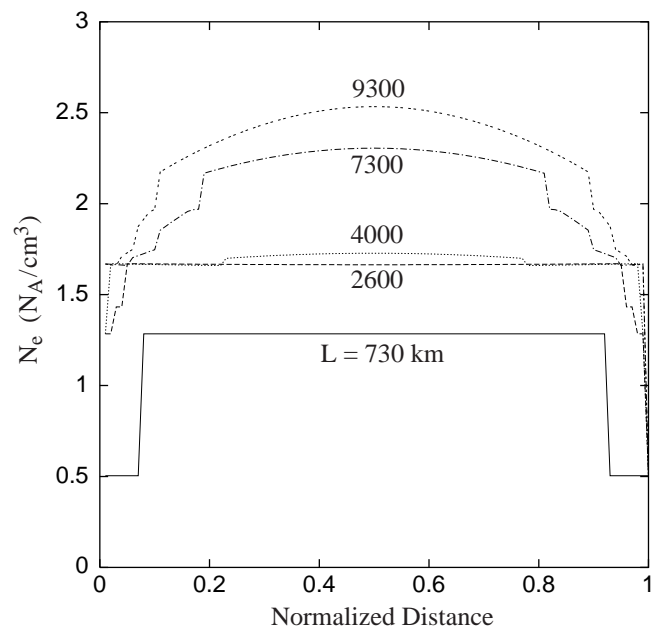


FIG. 15. Density profiles along a selection of chords of length L passing through the Earth; the horizontal axis is the fraction of the total path length.

REFERENCES

- [1] T. Toshito [Super-Kamiokande Collaboration], arXiv:hep-ex/0105023.
- [2] J. E. Hill [K2K Collaboration], arXiv:hep-ex/0110034.
- [3] M. Apollonio *et al.* [CHOOZ Collaboration], Phys. Lett. B **466**, 415 (1999) [arXiv:hep-ex/9907037].
- [4] F. Boehm *et al.*, Phys. Rev. D **64**, 112001 (2001) [arXiv:hep-ex/0107009].
- [5] The MINOS Collaboration, “*Neutrino Oscillation Physics at Fermilab: The NuMI-MINOS Project*”, Fermilab Report No. NuMI-L-375 (1998).
- [6] A. Rubbia for the ICARUS Collaboration, talk given at Skandinavian Neutrino Workshop (SNOW), Uppsala, Sweden, February (2001), which are available at <http://pcno-meth4.cern.ch/publicpdf.html>.
- [7] OPERA Collaboration, *Experiment Proposal OPERA: An appearance experiment to search $\nu_\mu \rightarrow \nu_\tau$ oscillations in the CNGS neutrino beam*, CERN/SPSC 2000-028, SPSC/P318, LNGS P25/2000, July, 2000.
- [8] V. Barger, A. M. Gago, D. Marfatia, W. J. Teves, B. P. Wood and R. Z. Funchal, arXiv:hep-ph/0110393.
- [9] J. N. Bahcall, M. H. Pinsonneault and S. Basu, Astrophys. J. **555**, 990 (2001) [arXiv:astro-ph/0010346].
- [10] Q. R. Ahmad *et al.* [SNO Collaboration], Phys. Rev. Lett. **87**, 071301 (2001) [arXiv:nucl-ex/0106015].
- [11] V. Barger, D. Marfatia and K. Whisnant, arXiv:hep-ph/0106207; G.L. Fogli, E. Lisi, D. Montanino and A. Palazzo, Phys. Rev. D **64**, 093007 (2001) [arXiv:hep-ph/0106247]; A. Bandyopadhyay, S. Choubey, S. Goswami and K. Kar, Phys. Lett. B **519**, 83 (2001) [arXiv:hep-ph/0106264]; P. I. Krastev and A. Y. Smirnov, arXiv:hep-ph/0108177. J. N. Bahcall, M. C. Gonzalez-Garcia and C. Pena-Garay, arXiv:hep-ph/0111150; M. V. Garzelli and C. Giunti, arXiv:hep-ph/0111254; P. Aliani, V. Antonelli, M. Picariello, and E. Torrente-Lujan, arXiv:hep-ph/0111418.
- [12] P. Alivisatos *et al.*, STANFORD-HEP-98-03; V. Barger, D. Marfatia and B. P. Wood, Phys. Lett. B **498**, 53 (2001) [arXiv:hep-ph/0011251].
- [13] C. Athanassopoulos *et al.* [LSND Collaboration], Phys. Rev. Lett. **81**, 1774 (1998) [arXiv:nucl-ex/9709006].
- [14] V. Barger, S. Geer, R. Raja and K. Whisnant, Phys. Rev. D **63**, 113011 (2001) [arXiv:hep-ph/0012017]; B. Richter, arXiv:hep-ph/0008222;
- [15] S. Geer, Phys. Rev. D **57**, 6989 (1998) [Erratum-ibid. D **59**, 039903 (1998)] [arXiv:hep-ph/9712290]; V. Barger, S. Geer and K. Whisnant, Phys. Rev. D **61**, 053004 (2000) [arXiv:hep-ph/9906487]; T. Adams *et al.*, arXiv:hep-ph/0111030.
- [16] Y. Itow *et al.*, arXiv:hep-ex/0106019.
- [17] A. Cervera *et al.* Nucl. Phys. B **579**, 17 (2000) [Erratum-ibid. B **593**, 731 (2000)] [arXiv:hep-ph/0002108].
- [18] M. Freund, Phys. Rev. D **64**, 053003 (2001) [arXiv:hep-ph/0103300].
- [19] V. Barger, K. Whisnant, S. Pakvasa and R. J. Phillips, Phys. Rev. D **22**, 2718 (1980).
- [20] T. K. Kuo and J. Pantaleone, Rev. Mod. Phys. **61**, 937 (1989).
- [21] V. Barger, K. Whisnant and R. J. Phillips, Phys. Rev. Lett. **45**, 2084 (1980); S. Pakvasa in *High Energy Physics-1980*, edited by L. Durand and L. Pondrom, AIP Conf. Proc. No. 68 (AIP, New York, 1981), p. 1164.

- [22] H. Minakata and H. Nunokawa, *JHEP* **0110**, 001 (2001) [arXiv:hep-ph/0108085].
- [23] J. Burguet-Castell, M. B. Gavela, J. J. Gomez-Cadenas, P. Hernandez and O. Mena, *Nucl. Phys. B* **608**, 301 (2001) [arXiv:hep-ph/0103258].
- [24] V. Barger, S. Geer, R. Raja and K. Whisnant, *Phys. Lett. B* **485**, 379 (2000) [arXiv:hep-ph/0004208].
- [25] P. Lipari, *Phys. Rev. D* **61**, 113004 (2000) [arXiv:hep-ph/9903481].
- [26] V. Barger, D. Marfatia and K. Whisnant, arXiv:hep-ph/0108090.
- [27] W. J. Marciano, arXiv:hep-ph/0108181.
- [28] R. J. Geller and T. Hara, arXiv:hep-ph/0111342.
- [29] M. Freund, P. Huber and M. Lindner, *Nucl. Phys. B* **615**, 331 (2001) [arXiv:hep-ph/0105071]; J. Pinney and O. Yasuda, *Phys. Rev. D* **64**, 093008 (2001) [arXiv:hep-ph/0105087].
- [30] A. Dziewonski and D. Anderson, *Phys. Earth Planet. Inter.* **25**, 297 (1981).